►Aalborg University

One university – three campuses

AALBORG
– approximately **18,900** students and **2,900** staff

COPENHAGEN
– approximately **2,660** students and **715** staff

ESBJERG
– approximately **450** students and **46** staff

AAU Energy

Frede Blaabjerg's Group

Unlock Potentials of Multi-Sampling in Grid-Connected Voltage Source Converters

Shan He
Email: shanhe@ieee.org
Department of Energy
Aalborg University, Denmark

AAU ENERGY
AALBORG UNIVERSITY

▶Outline

- Introduction
- Multi-sampling PWM mechanism and ripple filter design
- Passivity-based multi-sampling current/voltage control
- Multi-sampling-based grid voltage estimation
- Summary

▶ Introduction

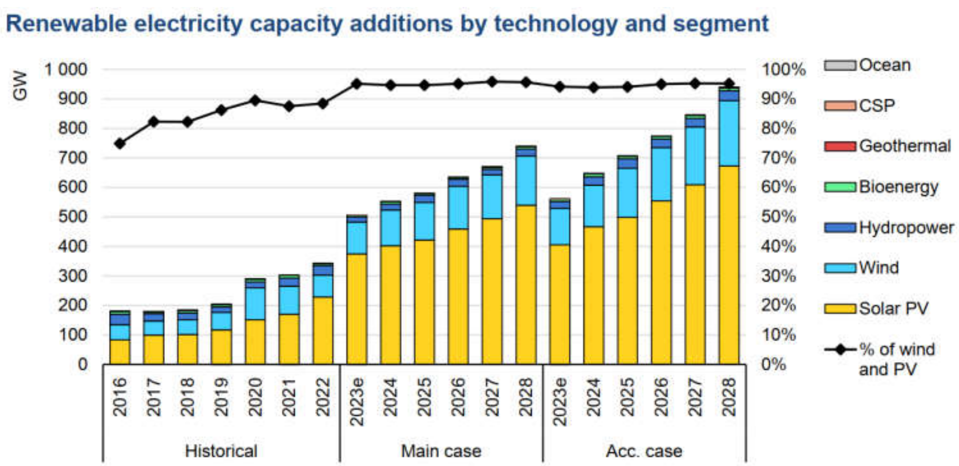

Renewable share of annual power capacity expansion[1]

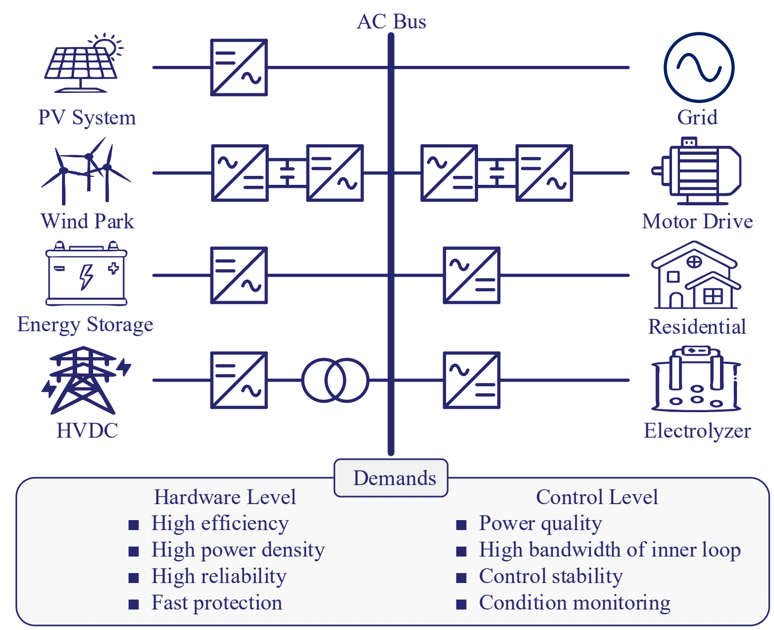

Applications and demands of VSCs in power system

Source: [1] IEA, "Renewable 2023 Analysis and forecast to 2028," *Tech. Rep.*, 2024.

▶ Introduction

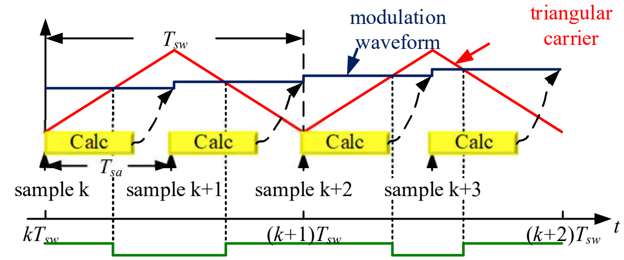

Double-sampling
($T_d = 1.5T_{sw}/2$)

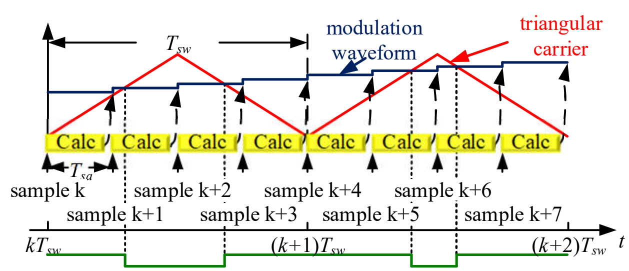

Multi-sampling
($T_d = 1.5T_{sw}/N$)

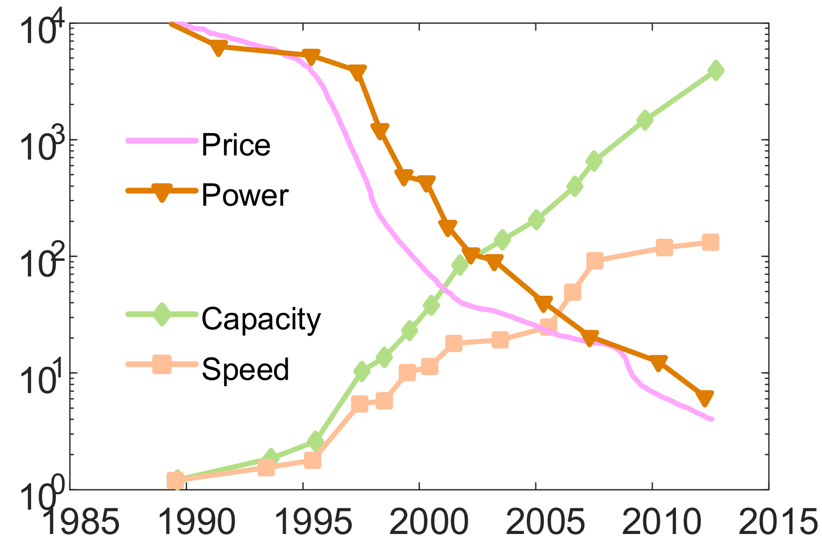

Xilinx FPGA development trend[1]

- ❑ Reduced control delay
- ❑ More information
- ❑ Decreasing cost of MCU

➔

- ➢ Improved stability
- ➢ Make converter smarter

Source: [1] S. Trimberger, “Three ages of FPGAs: A retrospective on the first thirty years of FPGA technology,” *Proc. IEEE.*, 2018.

▶ Introduction

Question 1: What is the internal mechanism of multi-sampling PWM?

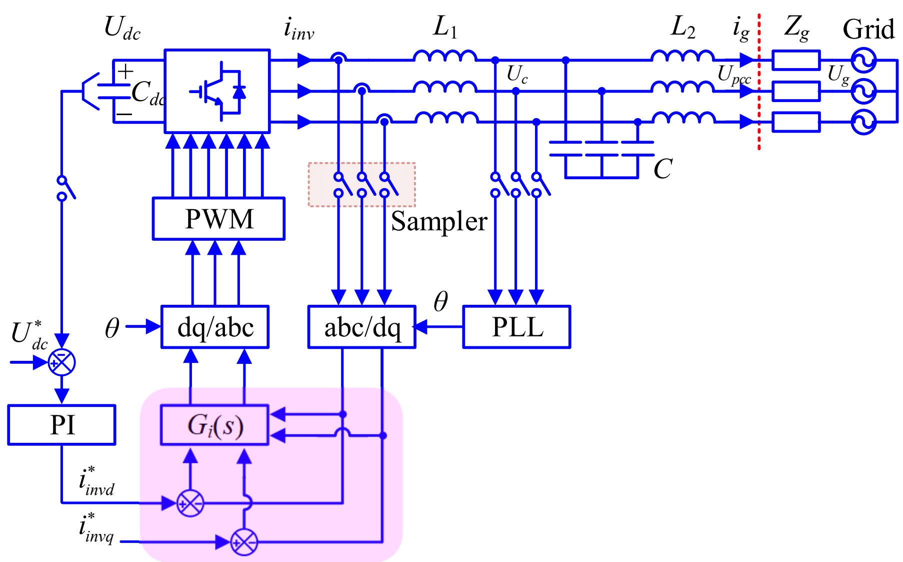

Typical control structure of a three-phase VSC

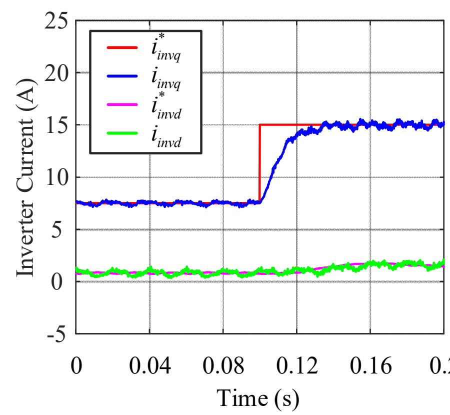

Double-sampling control

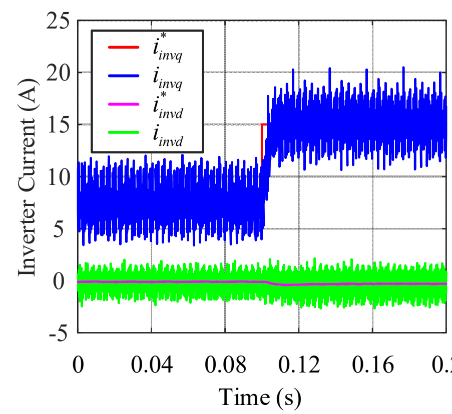

Eight-sampling control

❑ High-frequency switching harmonics

– Keep or remove?

Source: [1] S. He, *et.al*, "Aliasing suppression of multi-sampled current controlled LCL-filtered inverters," *IEEE JESTPE.*, 2022.

▶Introduction

Question 2: How to enhance control stability using multi-sampling?

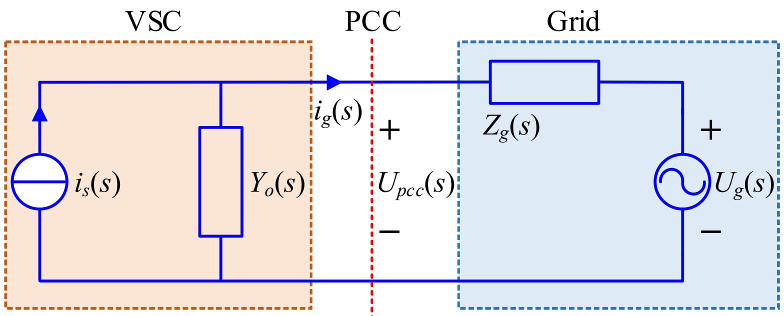

- ❑ Passivity-based admittance shaping
- – VSC-grid interactive stability is secured regardless of grid impedance

- ❑ $Y_o(j\omega)$ is passive at all frequencies
- – $Y_o(j\omega)$ is dissipative below Nyquist frequency

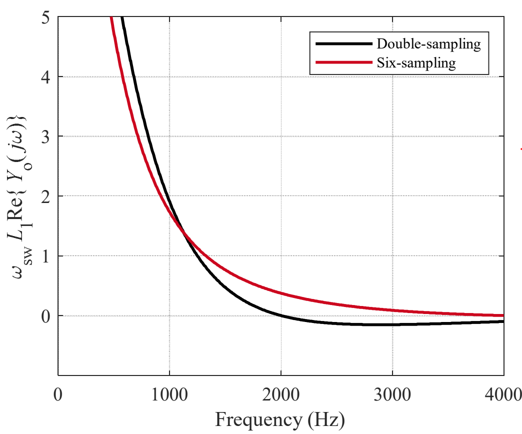

Re{$Y_o(j\omega)$} is non-negative

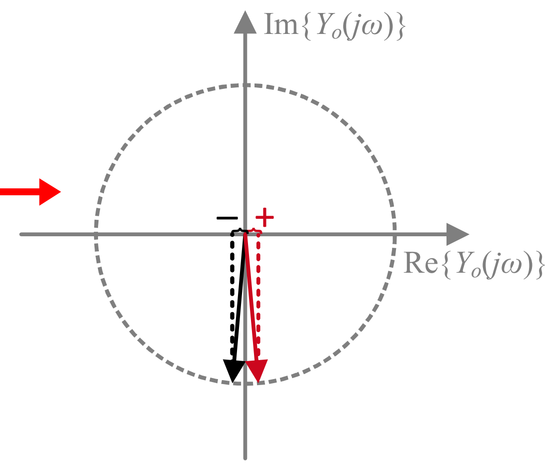

Phase of $Y_o(j\omega)$ is between [-90°, 90°]

Source: [1] L. Harnefors, *et.al*, "Passivity-based stability assessment of grid-connected VSCs—an overview," *IEEE JESTPE.*, 2015.

▶ Introduction

Question 3: How to utilize multi-sampling for condition monitoring?

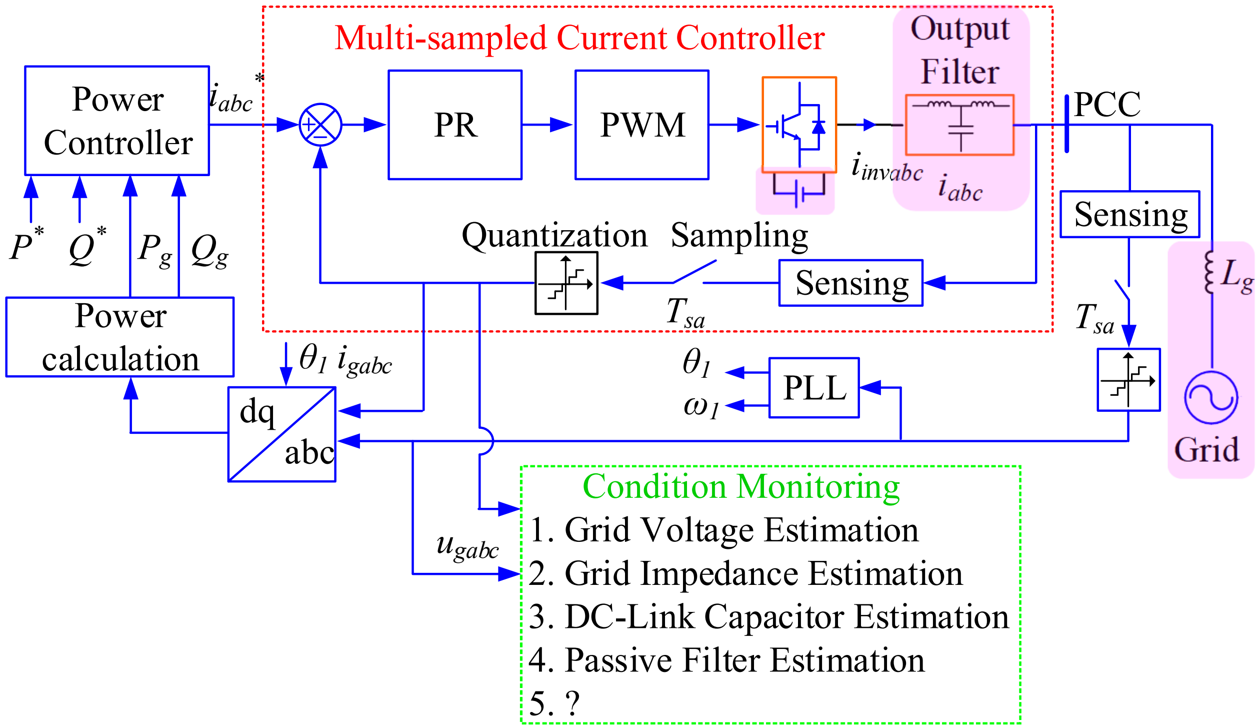

Source: [1] S. He, *et.al*, "A review of multisampling techniques in power electronics applications," *IEEE TPEL.*, 2022.

▶ Outline

- Introduction
- Multi-sampling PWM mechanism and ripple filter design
- Passivity-based multi-sampling current/voltage control
- Multi-sampling-based grid voltage estimation
- Summary

►Multi-Sampling PWM Mechanism

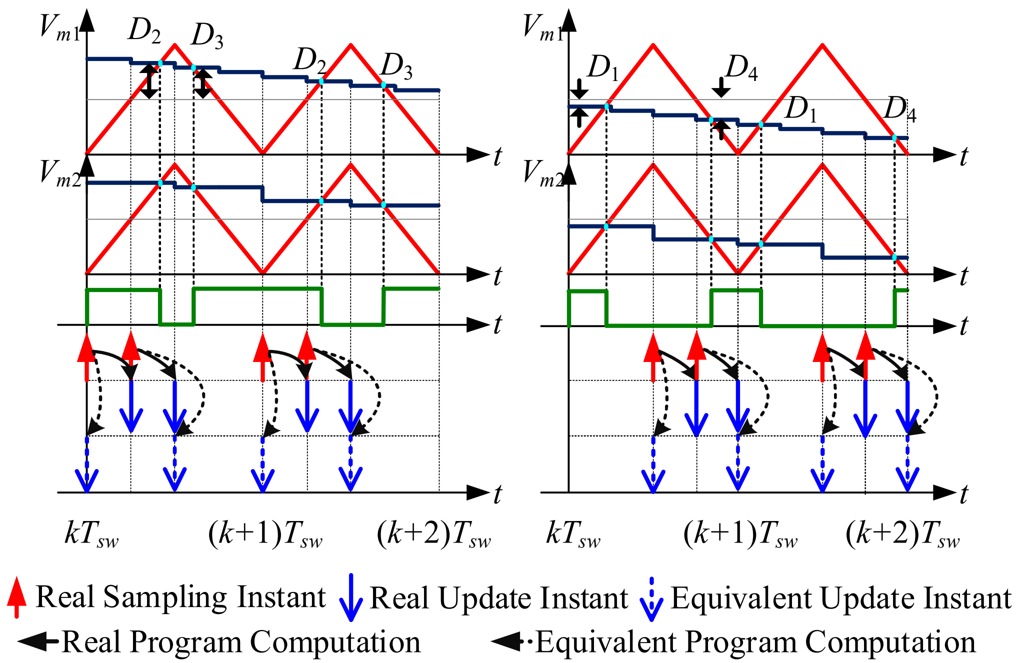

Positive half cycle　　Negative half cycle

D_2: zero computation delay

D_3: T_{sw}/4 computation delay

D_4: zero computation delay

D_1: T_{sw}/4 computation delay

Four-sampling control

↓

Double-sampling control with sampling instant shift

↓

Low-frequency aliasing

↓

Remove sampled switching harmonics

Total control delay:

→ $\underbrace{(1/4+0)/2}_{\text{Average computation delay}} + \underbrace{1/4}_{\text{PWM delay}} = 1.5T_{sw}/4$

▶ Multi-Sampling PWM Mechanism

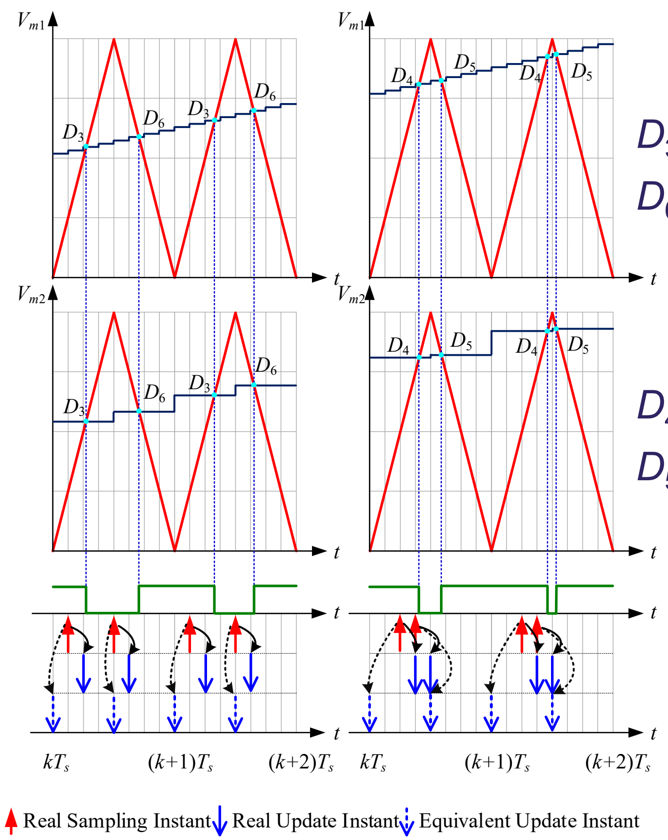

Positive half cycle

D_3: $-T_{sw}/8$ computation delay

D_6: zero computation delay

Total control delay:

$$\underbrace{(-1/8+0)/2}_{\text{Average computation delay}} + \underbrace{1/4}_{\text{PWM delay}} = 1.5T_{sw}/8$$

D_4: $-T_{sw}/8$ computation delay

D_5: zero computation delay

$$\underbrace{(-2/8+1/8)/2}_{\text{Average computation delay}} + \underbrace{1/4}_{\text{PWM delay}} = 1.5T_{sw}/8$$

Eight-sampling control → Double-sampling control with sampling instant shift

Low-frequency aliasing → Remove sampled switching harmonics

►Basic ripple filter design

$$RF(z)^{[1]} = \frac{(1+0.25)(1-(z^{-N}-\frac{1}{N}\sum_{n=1}^{N} z^{-n}))}{1-(z^{-N}-\frac{1}{N}\sum_{n=1}^{N} z^{-n})+0.25} \approx 1$$

$$SRF(z)^{[2]} = \frac{1}{2}(1+z^{-N/2}) \approx z^{-\frac{N}{4}}$$

$$MAF(z) = \frac{1}{N}\sum_{k=0}^{N-1} z^{-k} \approx z^{-\frac{N}{2}}$$

$$CMAF(z) = \frac{2}{N}(1+z^{-2}+z^{-4}+\cdots z^{-(N-2)}) \approx z^{-\frac{2N-4}{4}}$$

$$IRF(z)^{[3]} = CMAF(z)\underbrace{(3\log_2 N(1-z^{-1})-7+8z^{-1})}_{\text{Linear delay compensation}} \approx z^{-\frac{N}{4}}$$

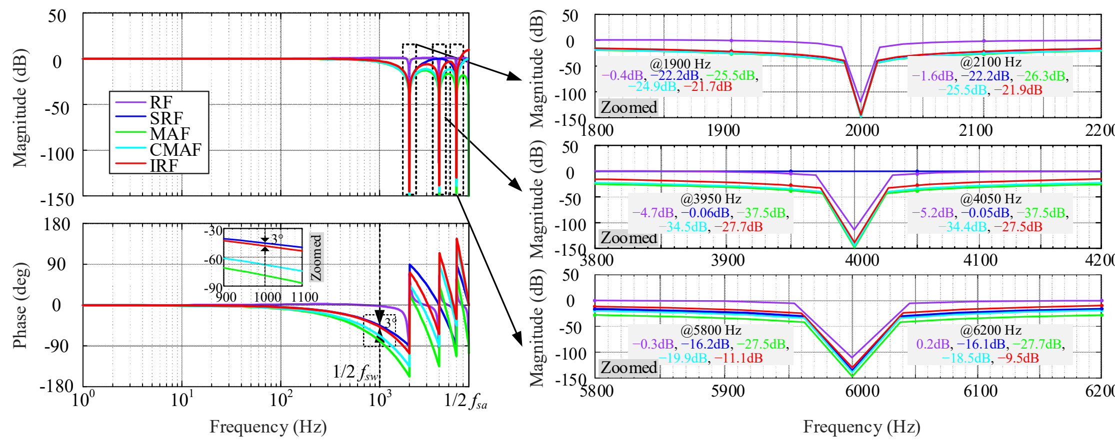

Bode diagram of repetitive filters based on eight-sampling (RF: repetitive filter, SRF: simplified repetitive filter, MAF: moving average filter, CMAF: compromised moving averaging filter, IRF: improved repetitive filter).

❑ Filter design objective: good filtering ability and small delay

➢ MAF has the best filtering ability but the introduced delay is large;

➢ IRF introduces similar delay with SRF and better filtering ability.

Source: [1] L. Corradini, et.al, "High-bandwidth multisampled digitally controlled DC–DC converters using ripple compensation," *IEEE TIE.*, 2008.
[2] L. Corradini, et.al, "Analysis of multisampled current control for active filters," *IEEE TIA*, 2008.
[3] S. He, et.al, ''Aliasing suppression of multi-sampled current controlled LCL-filtered inverters,'' *IEEE JESTPE*, 2022.

▶Basic ripple filter design

- ❑ Eight-sampling control without filter

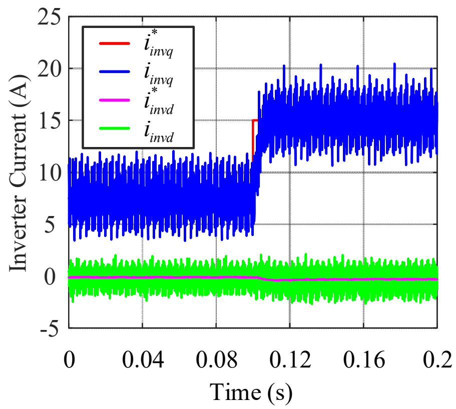

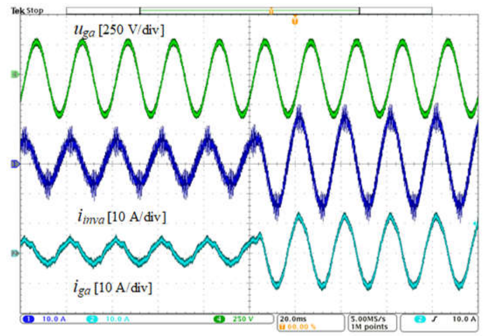

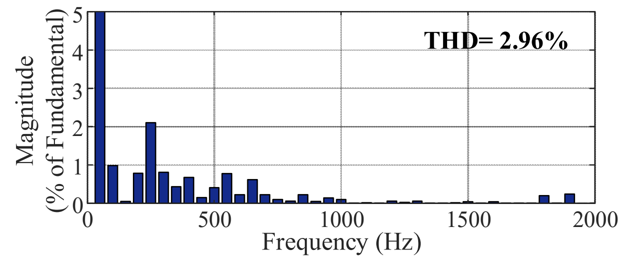

- ❑ Eight-sampling control with improved repetitive filter

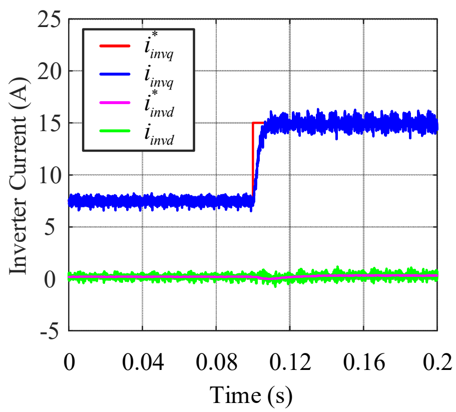

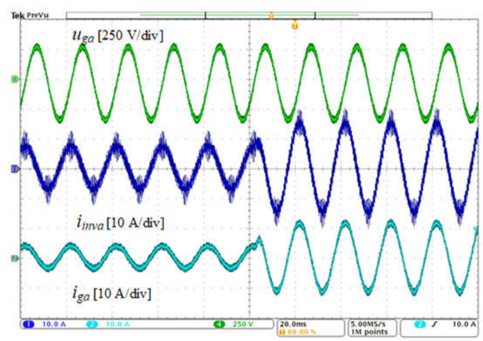

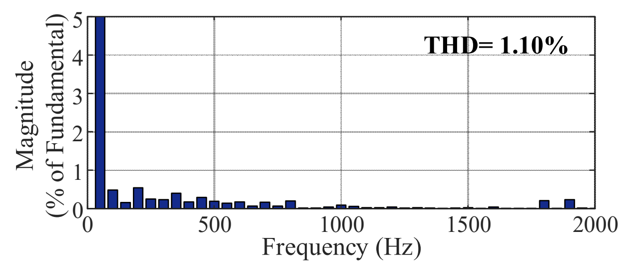

►Extended ripple filter design with less noise

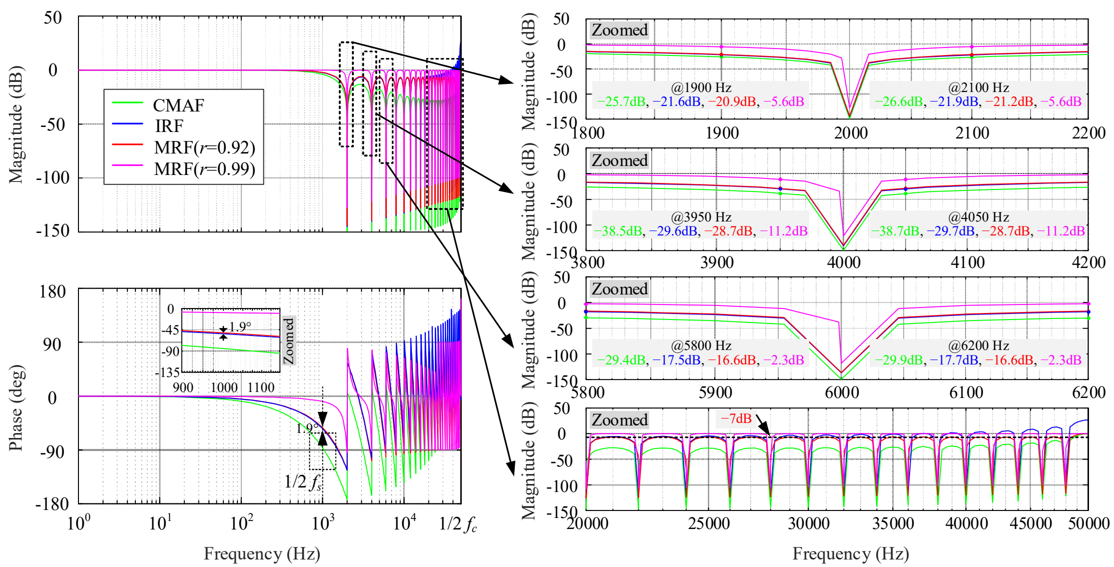

Bode diagram of the repetitive filters with a high-sampling rate (CMAF: compromised moving averaging filter, IRF: improved repetitive filter, MRF: modified repetitive filter, f_{sw}=2 kHz, f_{sa}=100 kHz).

$$CMAF(z)=\frac{2}{N}(1+z^{-2}+z^{-4}+\cdots z^{-(N-2)})\approx z^{-\frac{2N-4}{4}}$$

$$IRF(z)=CMAF(z)\underbrace{(3\log_2 N(1-z^{-1})-7+8z^{-1})}_{\text{Lineardelaycompensation}}\approx z^{-\frac{N}{4}}$$

$$MRF(z)^{[1]}=CMAF(z)\underbrace{\frac{1-r^N}{1-r^2}\frac{1-r^2z^{-2}}{1-r^Nz^{-N}}}_{\text{Delay Compensator}}$$

$$\approx z^{-\frac{N}{4}}(0<r<1)$$

- ❑ MRF can suppress noise around Nyquist frequency and similar deday with IRF

Source: [1] S. He, et.al, ‘‘Line voltage sensorless control of grid-connected inverters using multisampling,’’ *IEEE TPEL*, 2022.

►Ripple filter design considering topologies

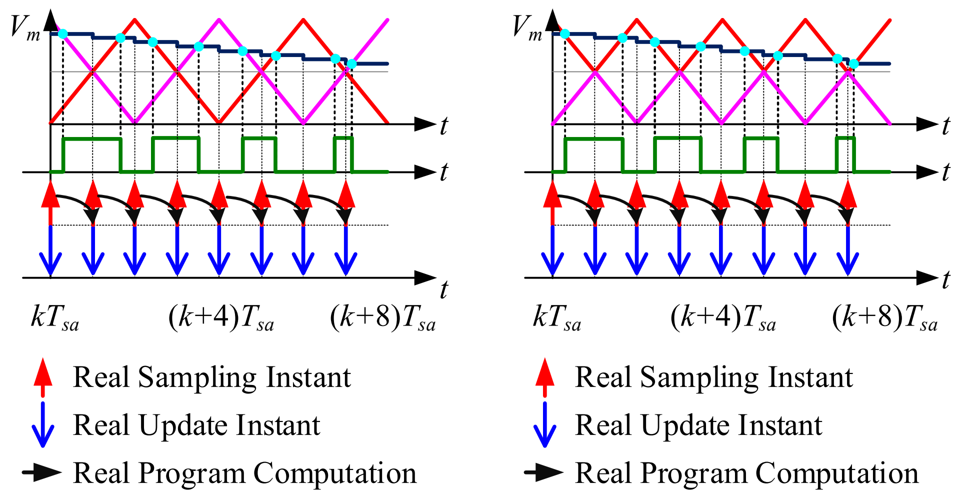

Four-sampling PWM for a single-phase H-bridge converter. (a) Seen from a preset switching frequency perspective, (b) Seen from an apparent switching frequency perspective.

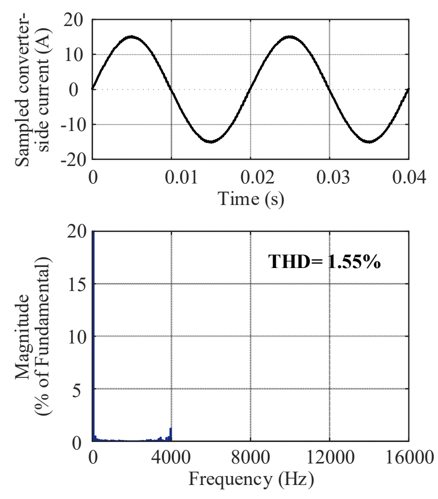

Four-sampled converter-side current (f_{sw}=4 kHz)

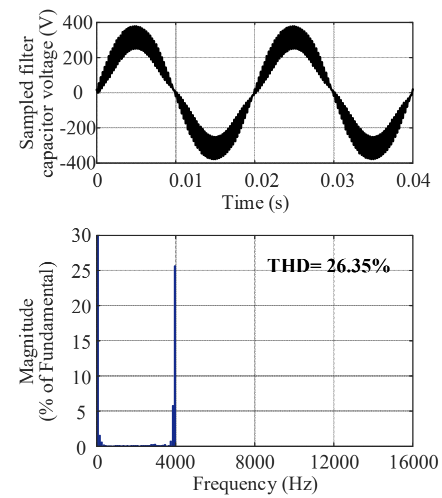

Four-sampled filter capacitor voltage

- ❑ Only ripple-free current can be acquired with four-sampling
- ❑ Multi-sampling rate selection should be based on apparent switching frequency

Source: [1] S. He, et.al., "Passivity-based multi-sampled converter-side current control of LCL-filtered grid-connected VSCs, " *IEEE TPEL, 2022.*
[2] J. Ma, et.al., "Multisampling method for single-phase grid-connected cascaded H-bridge inverters, " *IEEE TIE, 2020.*

►Ripple filter design considering topologies

COMPARISON AMONG VARIOUS MULTI-SAMPLED CONTROL METHODS FOR SINGLE/THREE-PHASE CONVERTERS

	Two-level VSC	Single-phase HB VSC	Single-phase CHB VSC
Sampling rate selection	N	$2N$	$2NM$
Loop delay	$(1.5/N+1/4)T_{sw}$	$(1.5/N+1/4)T_{ap\_sw}$	$(1.5/N+1/4)T_{ap\_sw}$

VSC: voltage source converter, HB: H-bridge, CHB: cascaded H-bridge, N: multi-sampling rate, M: number of cascaded cells, T_{sw}: switching period, T_{ap_sw}: apparent switching period, Loop Delay: computation delay, PWM delay, and anti-aliasing filter delay.

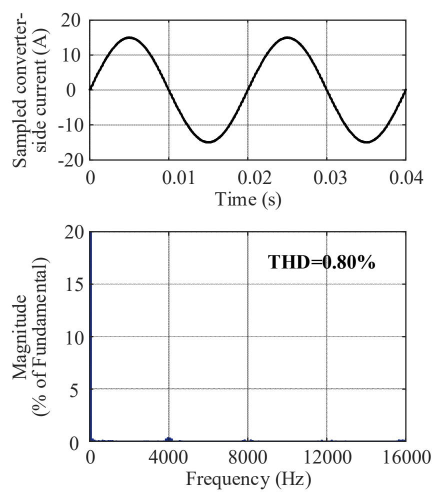

Sixteen-sampled converter-side current with MRF (f_{sw}=4 kHz)

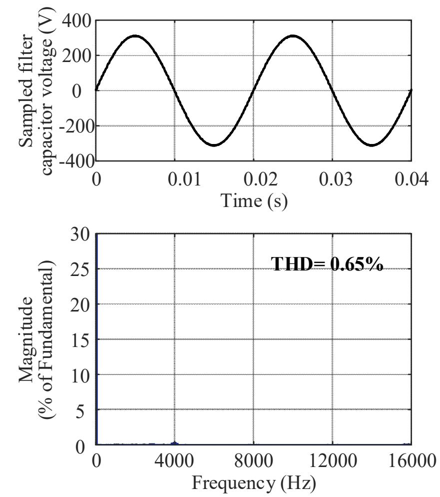

Sixteen-sampled filter capacitor voltage with MRF

- ❑ Multi-sampling with MRF can suppress the sampled voltage and current ripple;
- ❑ Sampling rate increases with the number of cascaded cells.

Source: [1] S. He, et.al., "Passivity-based multi-sampled converter-side current control of LCL-filtered grid-connected VSCs, " *IEEE TPEL, 2022.*

▶Outline

►Harmonic resonance

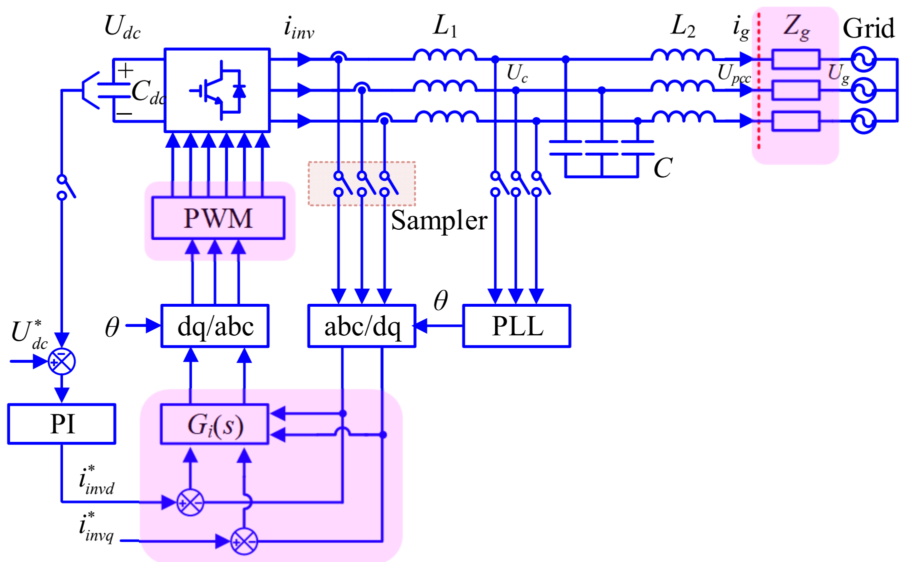

Typical control structure of a three-phase grid-following VSC

- ❑ Alternating current control (ACC) & control delay
- ❑ Grid impedance
- — High-frequency instability-main focus
- — Using multi-sampling

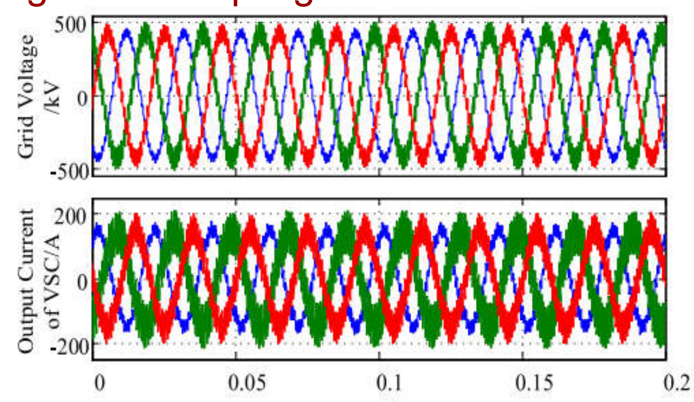

1270 Hz @ Southern Power Grid, China, 2017 [1]

►Passivity-Based Multi-Sampled Converter-Side Current Control

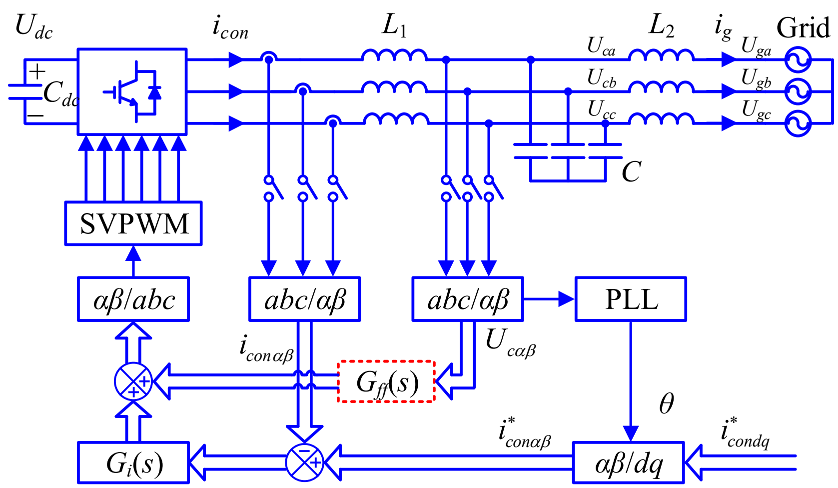

Three-phase control diagram

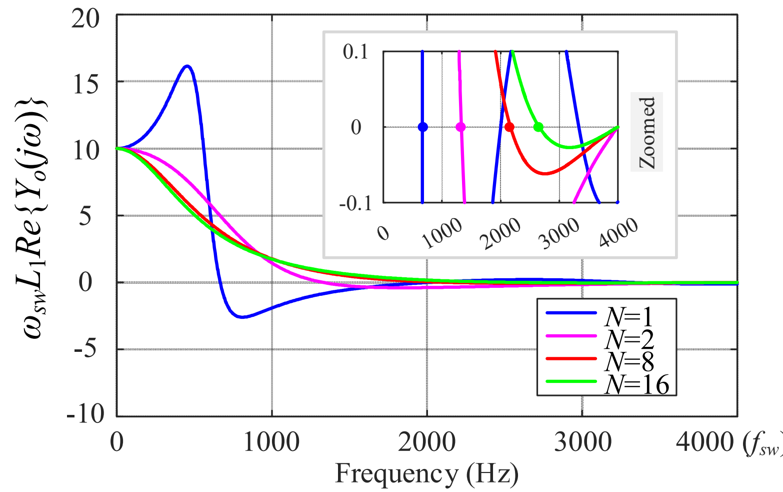

Real part of output admittance for single-loop control

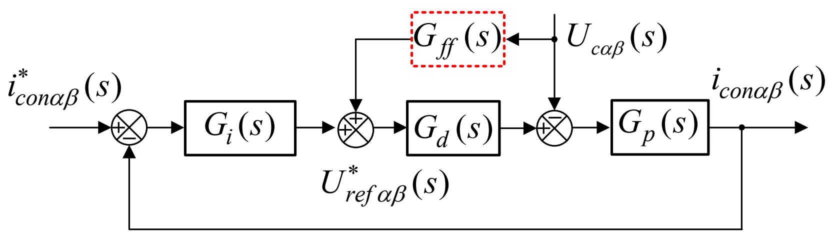

Current control model

$$\mathrm{Re}\{Y_o(j\omega)\} \approx \frac{K_p\cos(\omega T_d)}{(K_p\cos(\omega T_d))^2 + (\omega L_1 - K_p\sin(\omega T_d))^2}$$

$$f_{dissipative} = (0, \frac{1}{4T_d}) \Rightarrow T_d \le 0.25T_{sw}$$

- ❑ Multi-sampling control delay: $T_{d,MS} = (\frac{1}{4} + \frac{1.5}{N})T_{sw}$
- − Extra active damping is required

►Passivity-Based Multi-Sampled Converter-Side Current Control

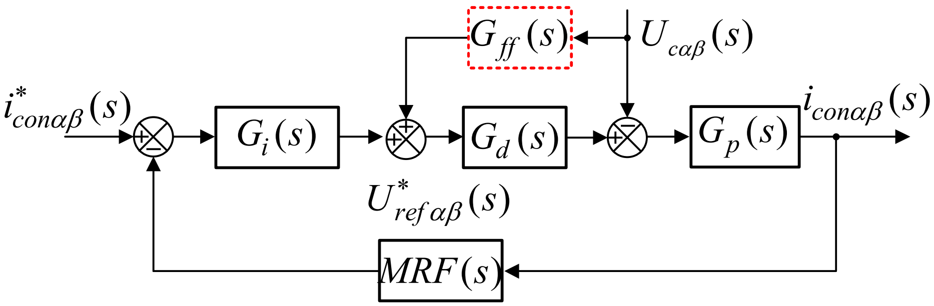

Control diagram of multi-sampled converter-side current control (MRF: modified repetitive filter)

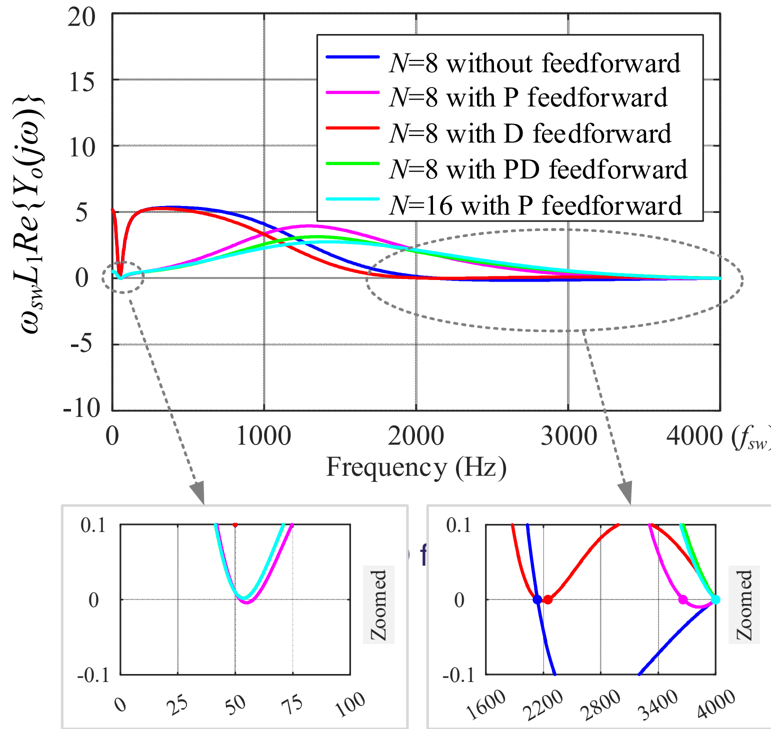

- ❑ Eight-sampling proportional-derivative capacitor voltage feedforward can achieve dissipativity;
- ❑ Derivative feedforward can be replaced by capacitor current feedforward if there is a noise issue.
- ❑ Sixteen-sampling capacitor voltage proportional feedforward can achieve dissipativity (Simple);

Source: [1] S. He et.al., "Passivity-based multi-sampled converter-side current control of LCL-filtered grid-connected VSCs," *IEEE TPEL*, 2022.

►Passivity-Based Multi-Sampled Converter-Side Current Control

VSC-grid interactive stability

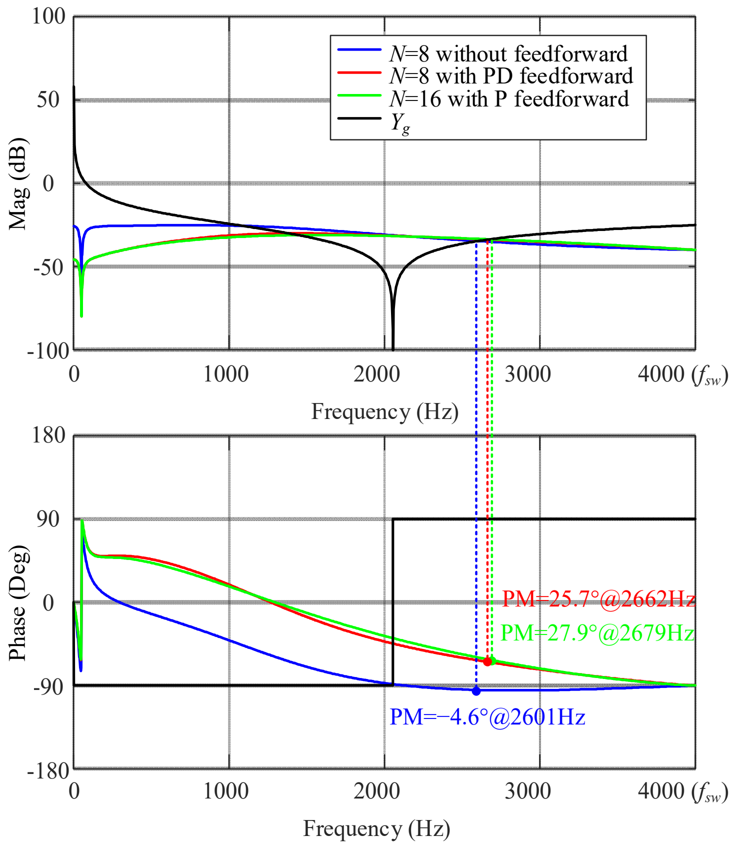

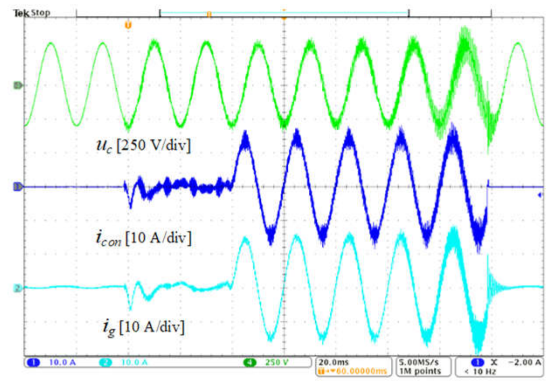

Eight-sampling without PD feedforward

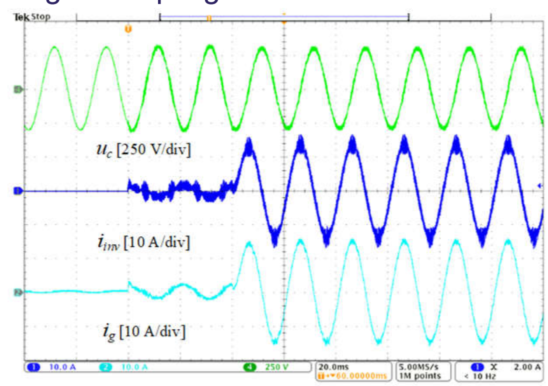

Eight-sampling with PD feedforward

►Comparison with double-sampling damping design

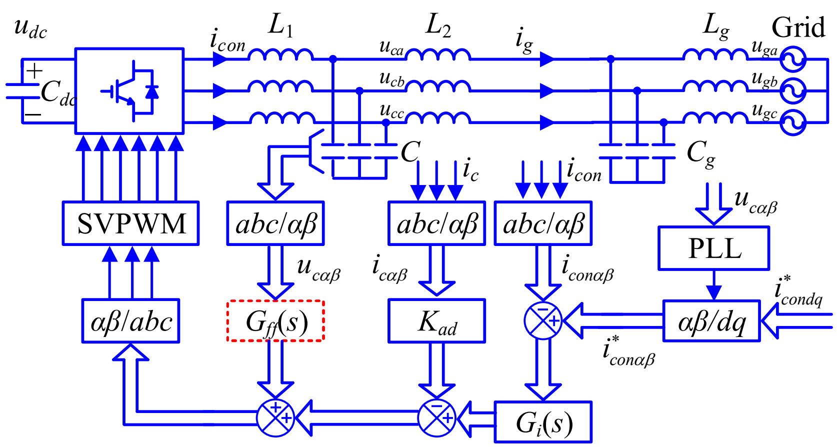

$$\begin{cases} K_{ad} = -\dfrac{4T_d^2 K_p}{\pi^2 L_{1n} C_n m^2} \\ G_{ff}(s) = K_{ff}(0.5 + 0.5e^{-sT_{sa}}) \end{cases}$$

- ❑ Capacitor current active damping and capacitor voltage feedforward should be carefully designed

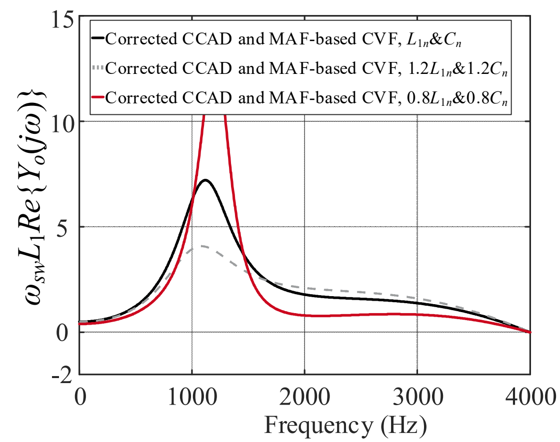

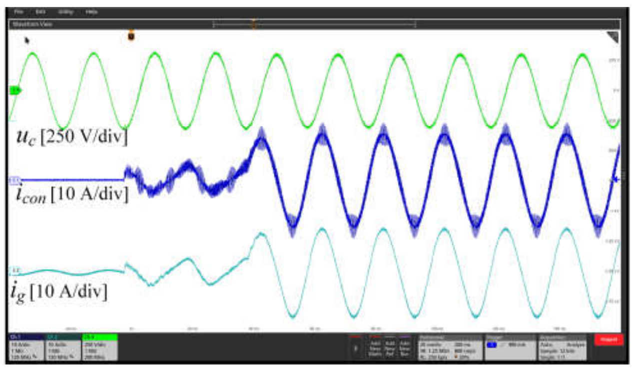

Source: [1] S. He et.al., "Design-oriented dissipativity robustness enhancement for current control of LCL-filtered grid-following VSCs," in *Proc. APEC*, 2023.

►Passivity-Based Multi-Sampled Grid-Side Current Control

Capacitor voltage feedforward and capacitor current active damping

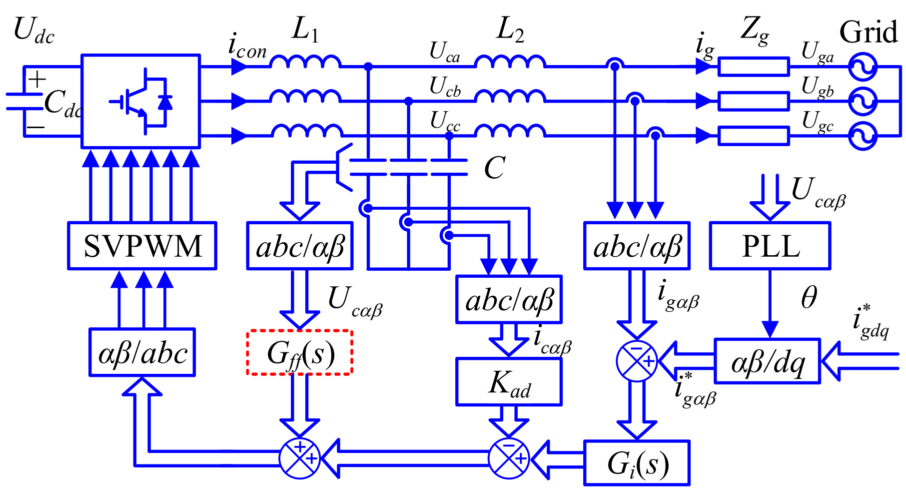

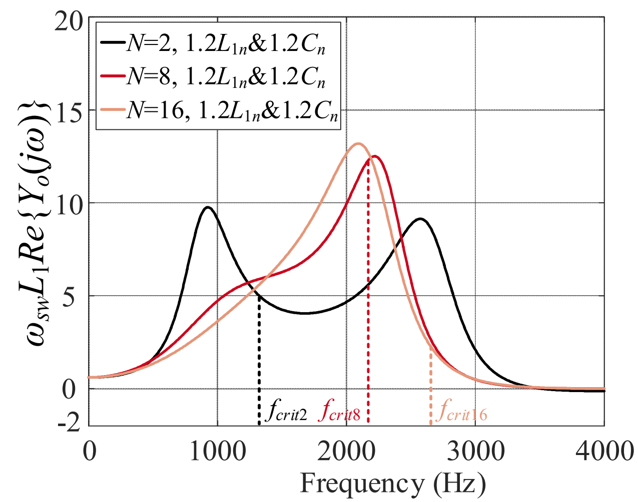

With parameter deviation

- ❑ Enhanced dissipativity robustness
- ❑ Dissipativity around switching frequency
- ❑ Transient currents during start-up and grid disturbance are suppressed

Source: [1] S. He, *et.al.*, "Dissipativity robustness enhancement for LCL-filtered grid-connected VSCs with multi-sampled grid-side current control," *IEEE TPEL.*, 2022 (Under review).

►Passivity-Based Multi-Sampled Grid-Side Current Control

Internal stability design ($G_{cl,g}(s)i_{ref}$)

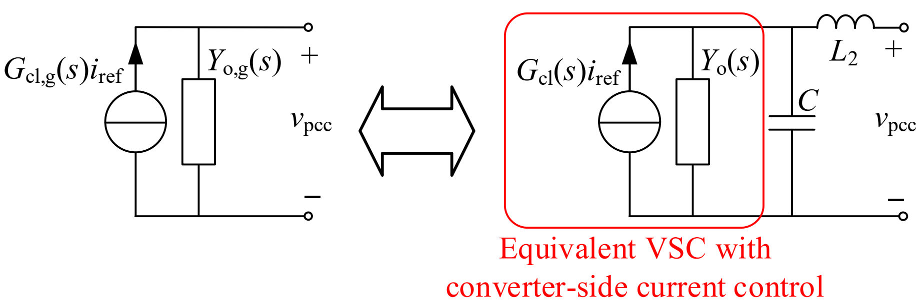

$$G_{cl,g}(s)i_{ref}(s) = \frac{1/(sL_2Y_o(s))}{1+Y_{CL_2}(s)/Y_o(s)}G_{cl}(s)i_{ref}(s)$$

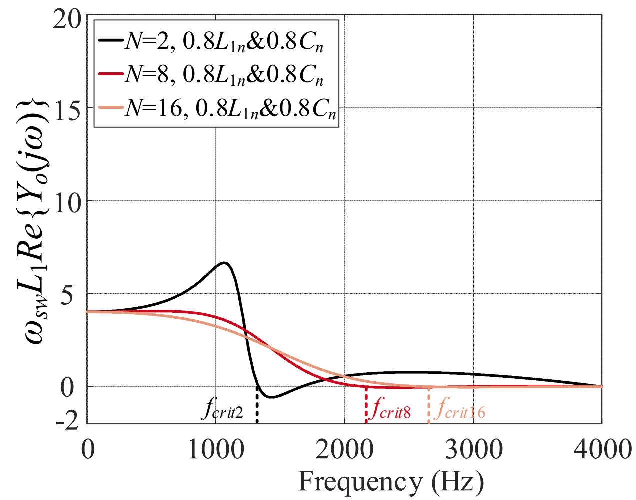

- ❑ $G_{cl}(s)$ is designed with a proper control bandwidth;
- ❑ $Y_o(s)/Y_{CL2}(s)$ determines internal stability
- • $Y_o(s)$ should be dissipative

❑ LCL-filter resonance frequency should be designed far away from critical frequency ($f_{sa}/6$) for capacitor current damping

►Passivity-Based Multi-Sampled Grid-Side Current Control

Internal stability design ($G_{cl,g}(s)i_{ref}$)

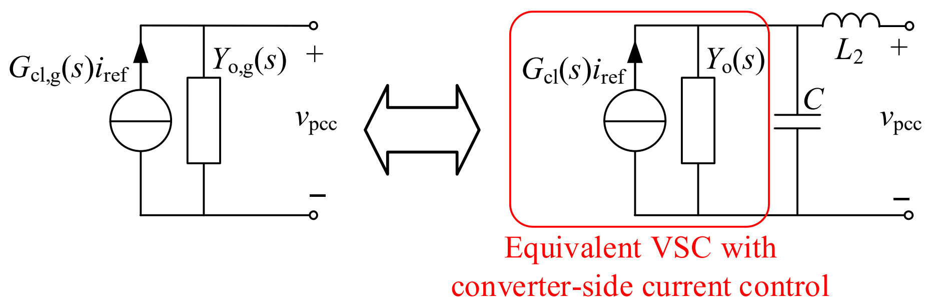

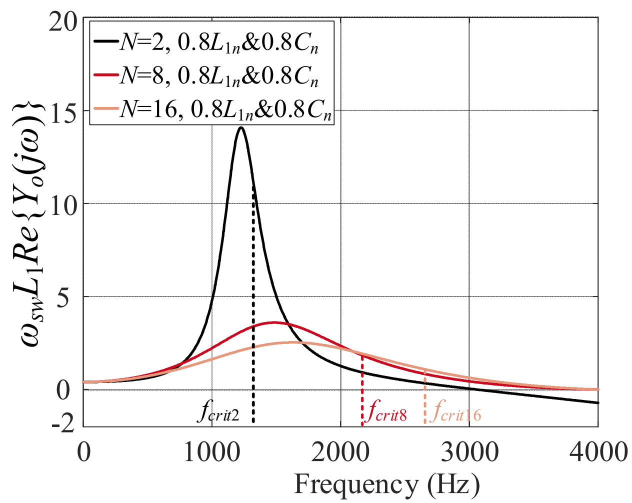

$$G_{cl,g}(s)i_{ref}(s) = \frac{1/(sL_2Y_o(s))}{1+Y_{CL_2}(s)/Y_o(s)}G_{cl}(s)i_{ref}(s)$$

- ❑ $G_{cl}(s)$ is designed with a proper control bandwidth;
- ❑ $Y_o(s)/Y_{CL2}(s)$ determines internal stability
- • $Y_o(s)$ should be dissipative

❑ Limit on LCL-filter resonance frequency design is removed by multi-sampling proportional capacitor voltage feedforward and capacitor current active damping

Source: [1] S. He, *et.al.*, "Dissipativity robustness enhancement for LCL-filtered grid-connected VSCs with multi-sampled grid-side current control," *IEEE TPEL.*, 2023.

►Passivity-Based Multi-Sampled Grid-Side Current Control

Internal stability

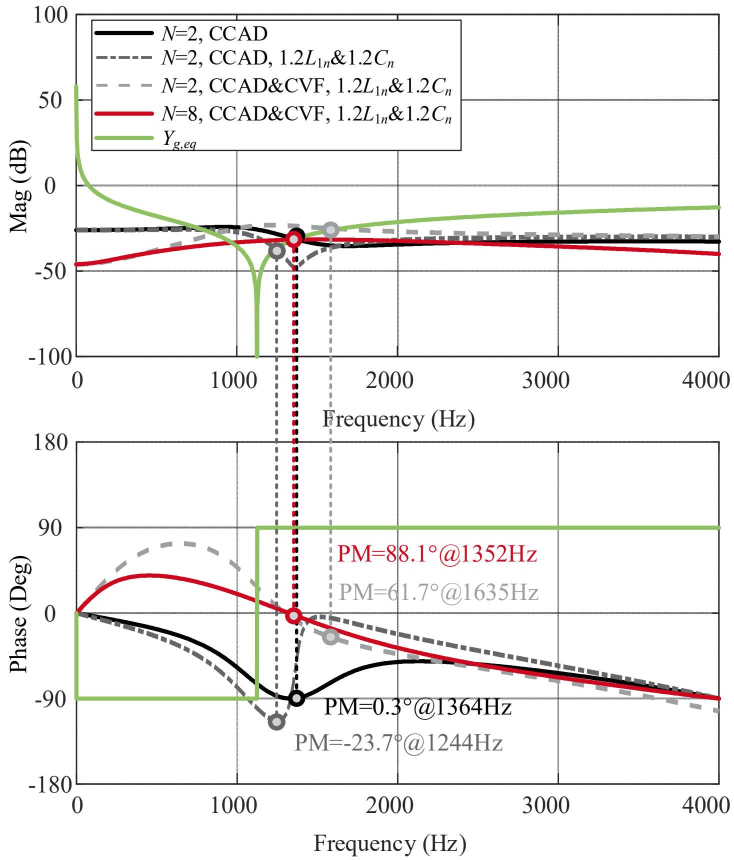

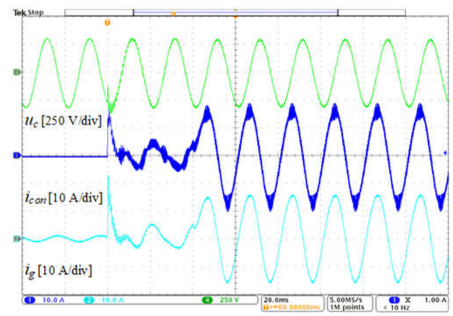

Double-sampling CCAD with nominal values of L_1 and C

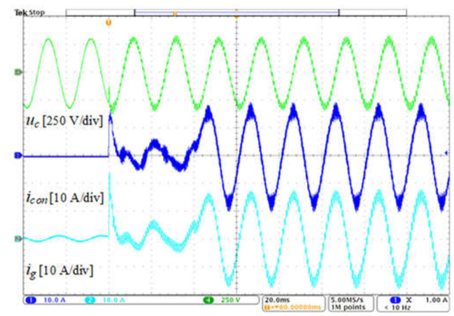

Double-sampling CCAD with +20% deviation of L_1 and C

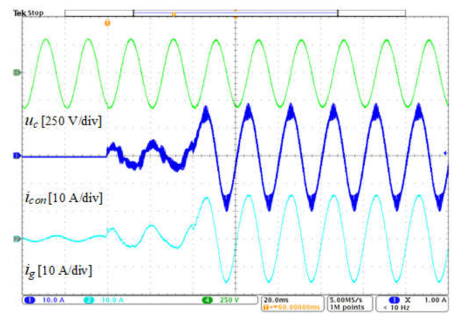

Double-sampling CCAD and CVF with +20% deviation of L_1 and C

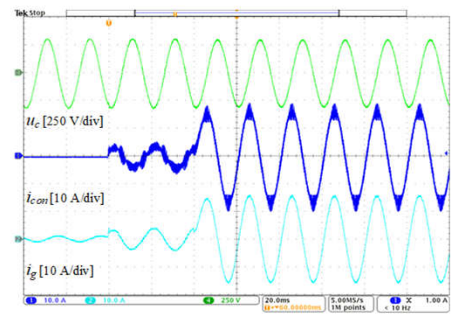

Eight-sampling CCAD and CVF with +20% deviation of L_1 and C

Source: [1] S. He, *et.al.*, "Dissipativity robustness enhancement for LCL-filtered grid-connected VSCs with multi-sampled grid-side current control," *IEEE TPEL.*, 2023.

► Passivity-Based Multi-Sampled Real-Time Current Control

Double-sampling real-time-update (DSRTU) PWM[1]

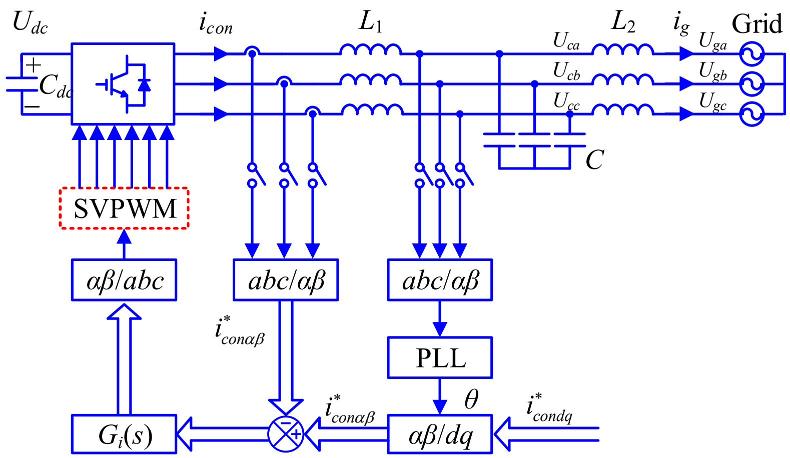

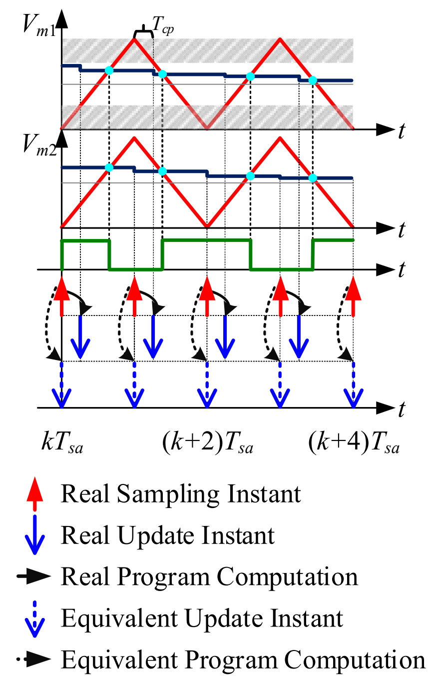

Without duty cycle limitation

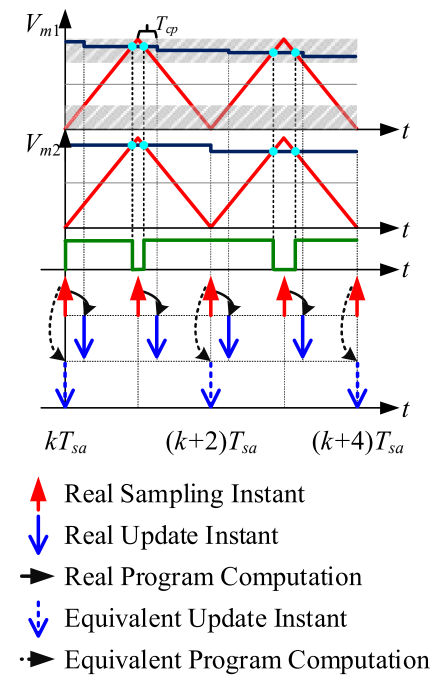

With duty cycle limitation

- Control delay:

$$\begin{cases} T_{d\_DSRTU} = \underbrace{0}_{\text{computation delay}} + \underbrace{0.25T_{sw}}_{\text{PWM delay}} = 0.25T_{sw} & d_{cri2} \le d \le d_{cri1} \\ T_{d\_DSRTU} = \underbrace{0}_{\text{computation delay}} + \underbrace{0.5T_{sw}}_{\text{PWM delay}} = 0.5T_{sw} & others \end{cases}$$

Source: [1] M. Hu, *et.al.*, "Fast current control without computational delay by minimizing update latency," *IEEE TPEL.*, 2021.

►Passivity-Based Multi-Sampled Real-Time Current Control

Enhanced real-time-update (ERTU) PWM using multi-sampling[1]

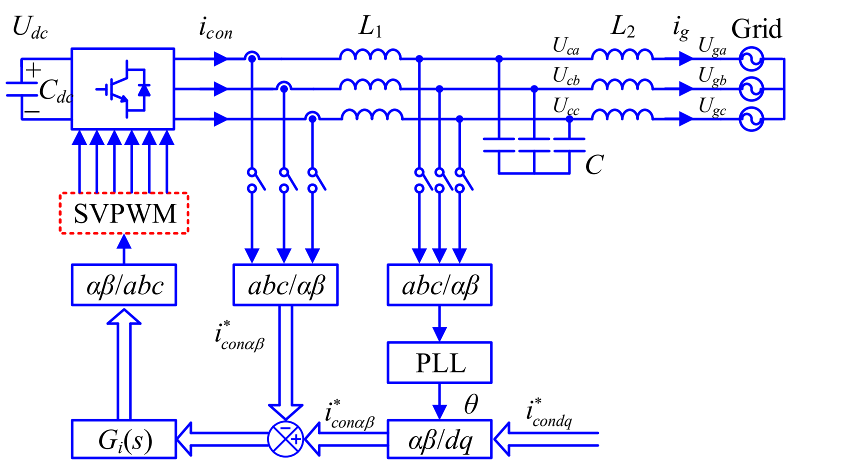

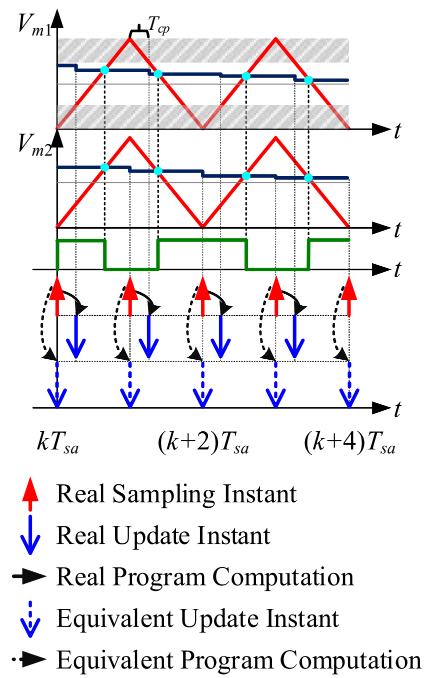

Without duty cycle limitation

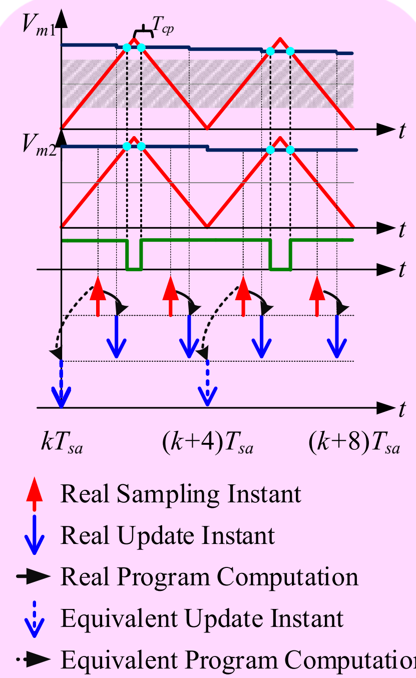

With duty cycle limitation

- Control delay:

$$\begin{cases} T_{d\_DSRTU} = \underbrace{0}_{\text{computation delay}} + \underbrace{0.25T_{sw}}_{\text{PWM delay}} = 0.25T_{sw} & d_{cri2} \le d \le d_{cri1} \\ T_{d\_DSRTU} = \underbrace{-0.25T_{sw}}_{\text{computation delay}} + \underbrace{0.5T_{sw}}_{\text{PWM delay}} = 0.25T_{sw} & \text{others} \end{cases}$$

Source: [1] S. He, *et.al* “Enhanced real-time-update current control of grid-connected VSCs using multi-sampling,” in *Proc. IEEE PEDG.*, 2022.

►Passivity-Based Multi-Sampled Real-Time Current Control

i_q^* changes from 15 A to -15 A (duty cycle slowly changes to the forbidden region)

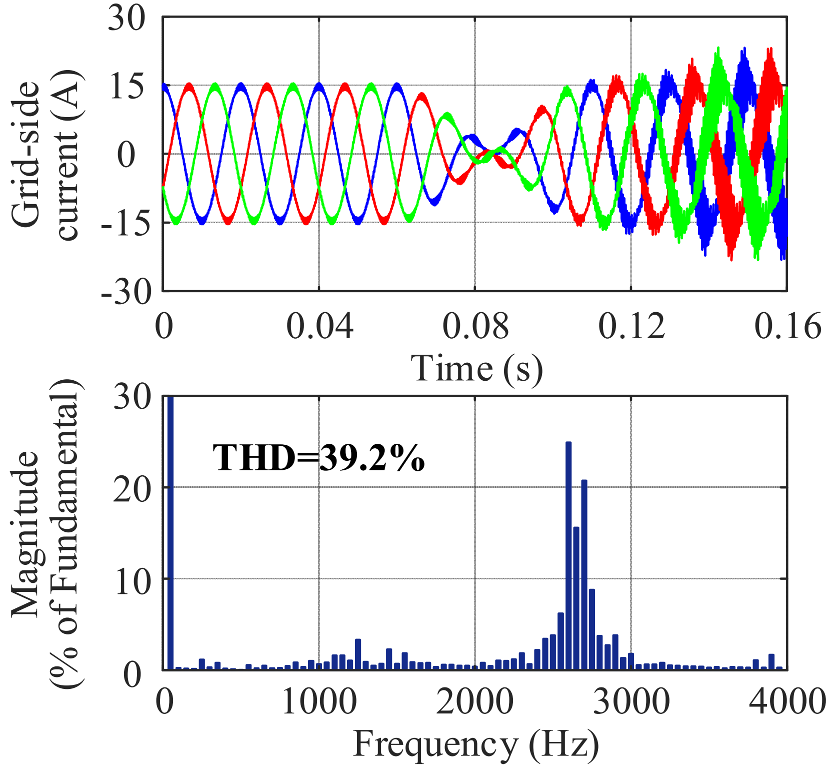

Double-sampling real-time-update PWM

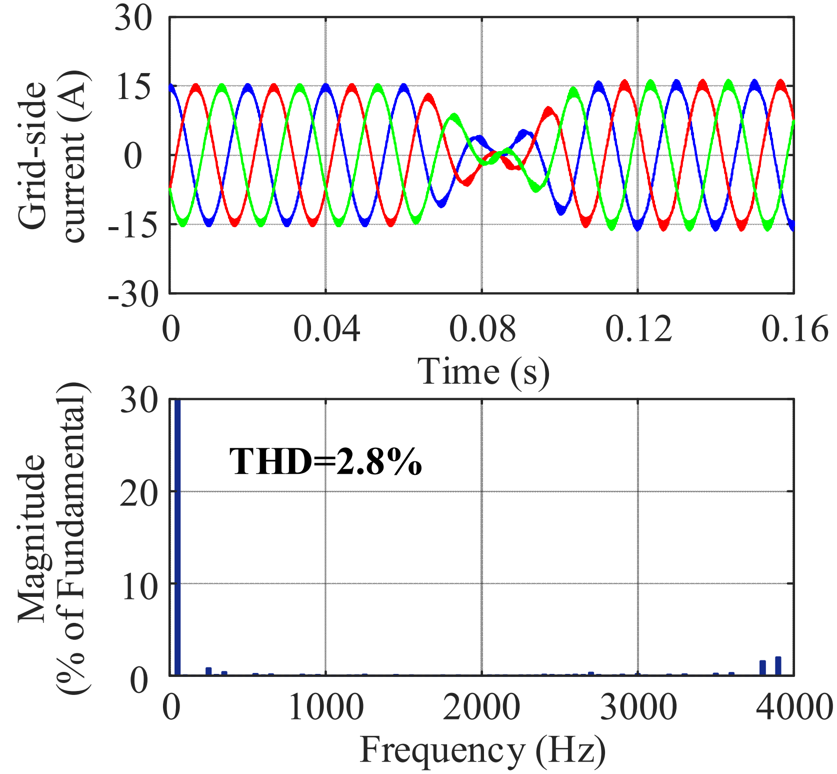

Enhanced real-time-update PWM

▶Passivity-Based Multi-Sampled Voltage Control

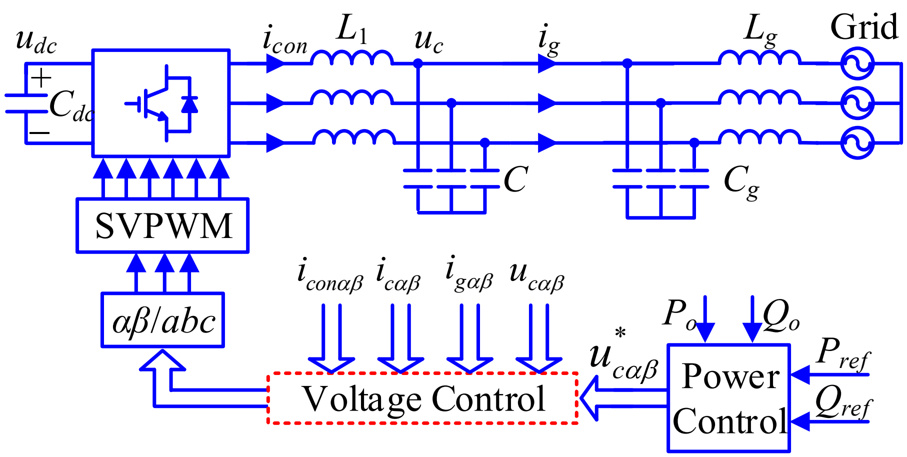

Control structure of a grid-forming VSC

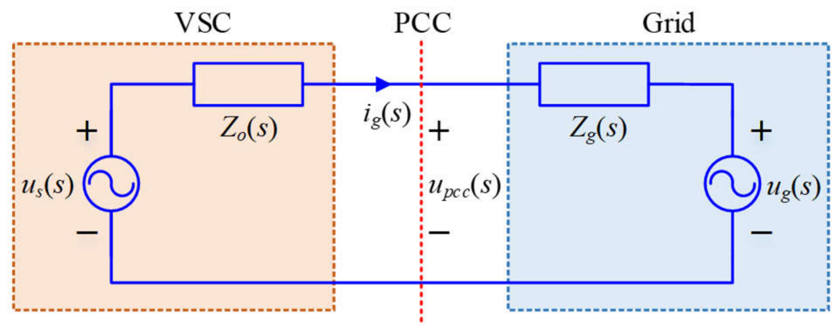

- ❑ Passivity-based impedance shaping
- – VSC-grid interactive stability is secured regardless of grid impedance

Due to control delay:

- ❑ Limit LC-filter design
- ❑ Weaken robustness against parameter deviation

- ❑ $Z_o(j\omega)$ is passive at all frequencies
- – $Z_o(j\omega)$ is dissipative below Nyquist frequency

►Passivity-Based Multi-Sampled Voltage Control

Without grid-side current feedforward (GSCF)

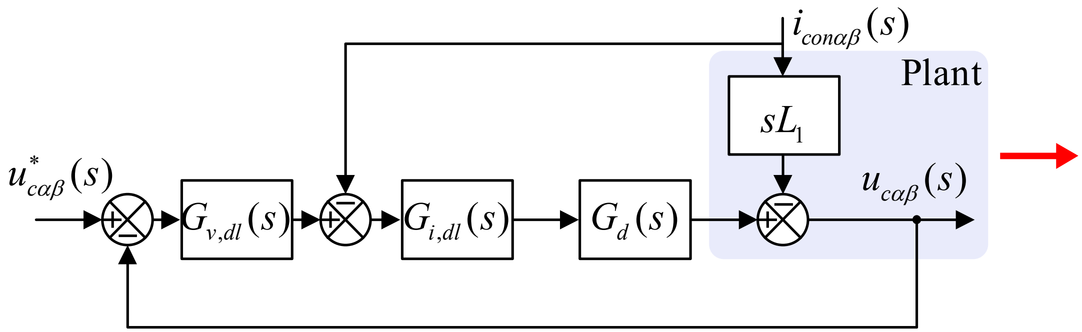

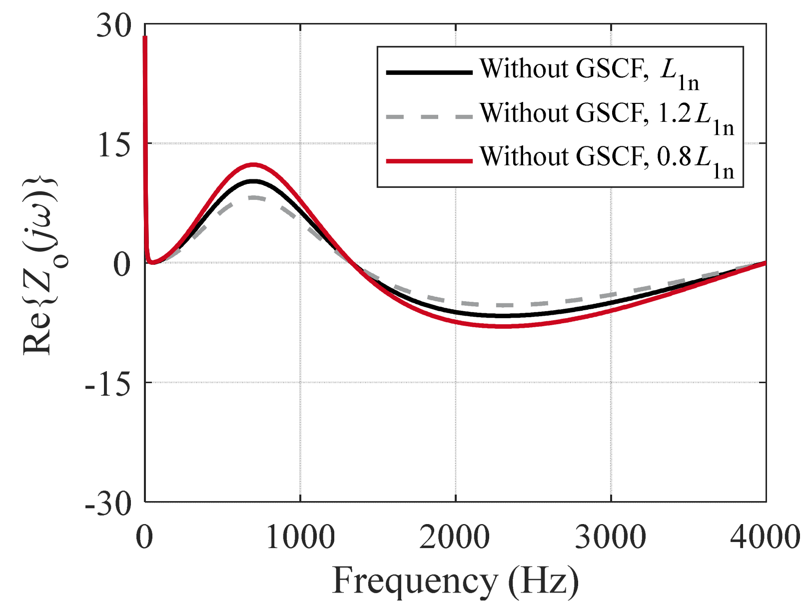

- ❑ Large non-dissipative area in the high-frequency region

$$f_{rn} < f_{crit} = \frac{1}{4T_d}$$

►Passivity-Based Multi-Sampled Voltage Control

With grid-side current feedforward (GSCF)

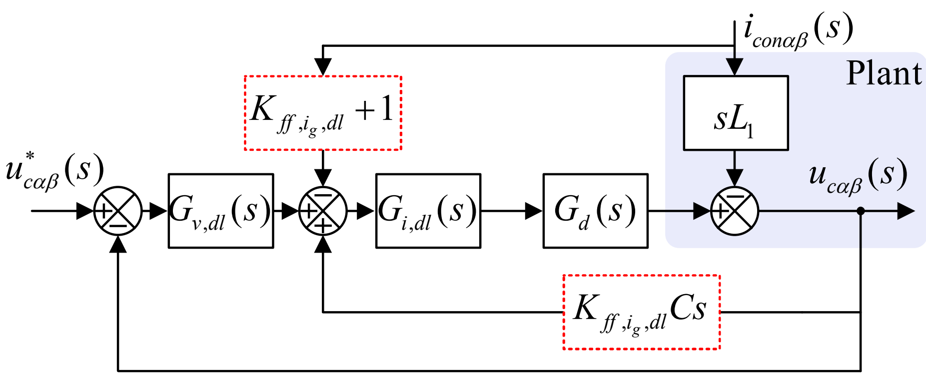

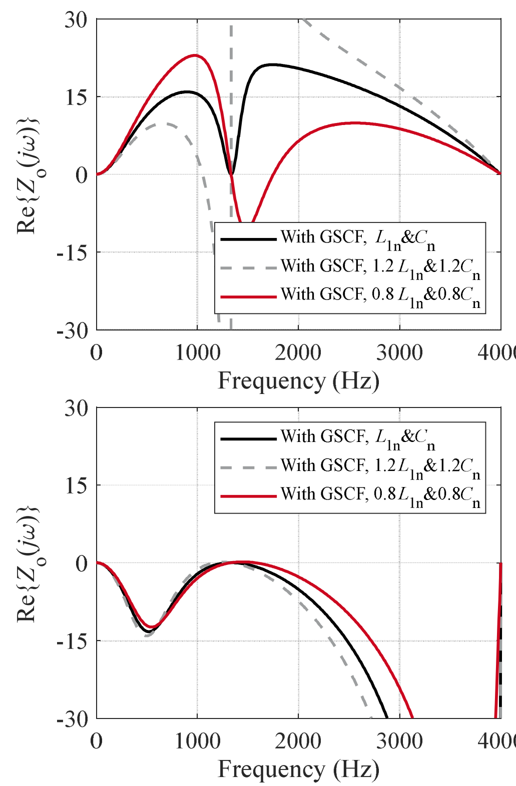

$$f_{rn} < f_{crit} = \frac{1}{4T_d}$$

$$f_{rn} > f_{crit} = \frac{1}{4T_d}$$

- ❑ LC-filter resonance frequency design is limited
- ❑ Weak robustness against parameter deviation

►Passivity-Based Multi-Sampled Converter-Side Current Control

With converter-side current, capacitor current feedforward, capacitor voltage feedforward

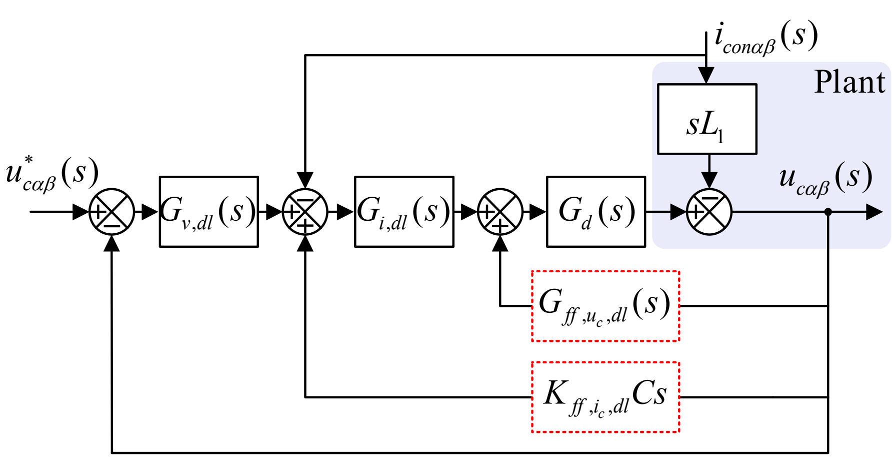

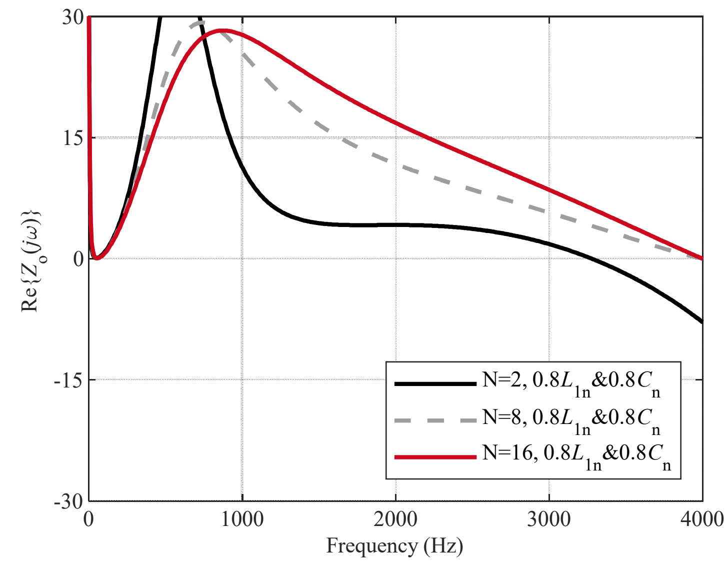

- ❑ LC-filter design limitation is removed
- ❑ Not sensitive to filter parameter deviation
- ❑ Capacitor current feedforward can be removed using 16-sampling

►Passivity-Based Multi-Sampled Voltage Control

f_{rn}> $f_{crit,N=2}$ & without filter parameter deviation

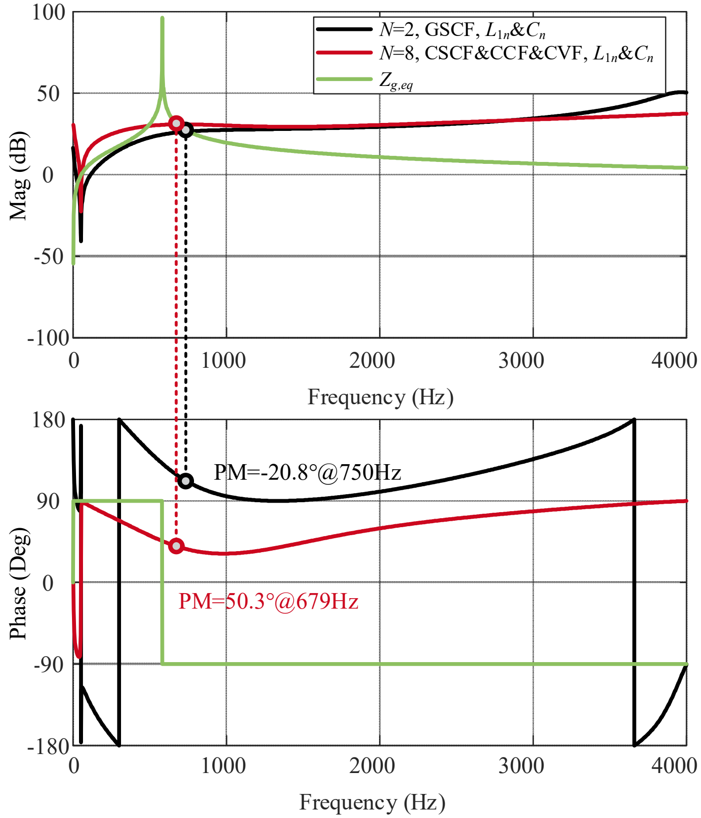

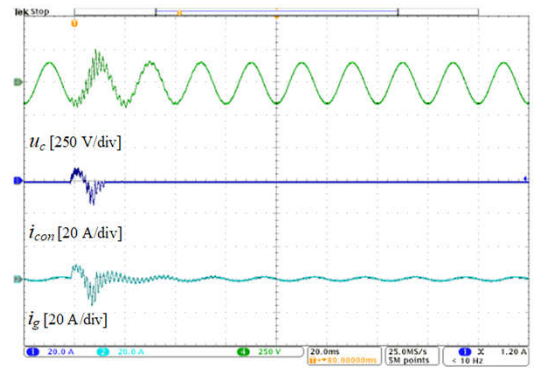

Double-sampling GSCF

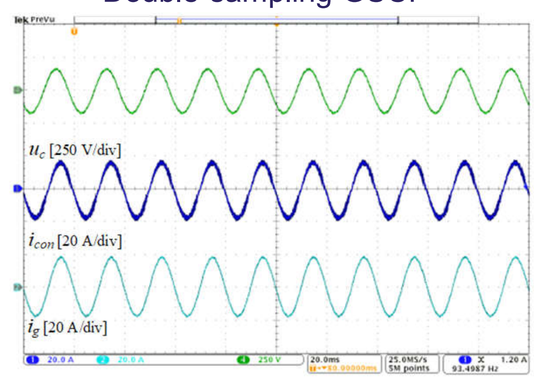

Eight-sampling CCAD, CSCAD, and CVF

►Passivity-Based Multi-Sampled Voltage Control

$f_r < f_{crit,N=2}$ & with -20% filter parameter deviation

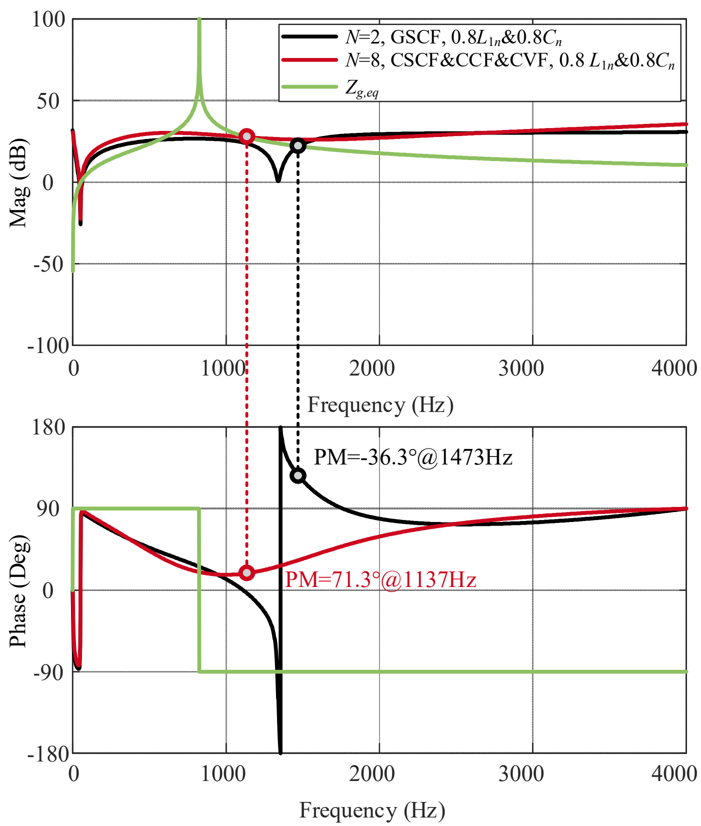

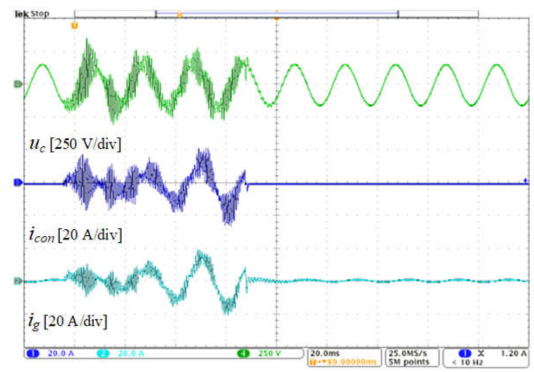

Double-sampling GSCF

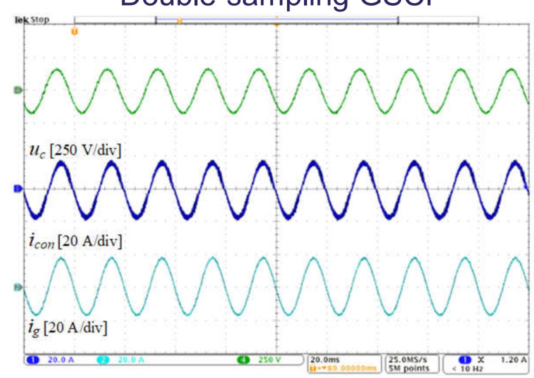

Eight-sampling CCAD, CSCAD, and CVF

▶ Outline

- ▶ Introduction
- ▶ Multi-sampling PWM mechanism and ripple filter design
- ▶ Passivity-based multi-sampling current/voltage control
- ▶ Multi-sampling-based grid voltage estimation
- ▶ Summary

► Multi-sampling-based grid voltage estimation

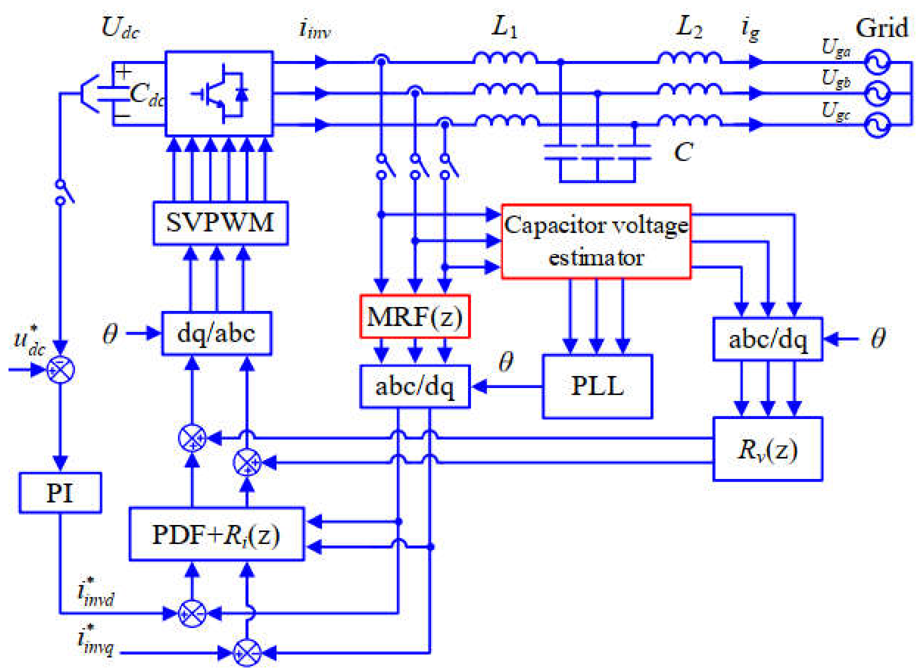

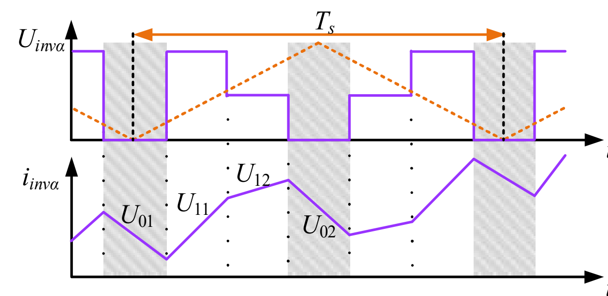

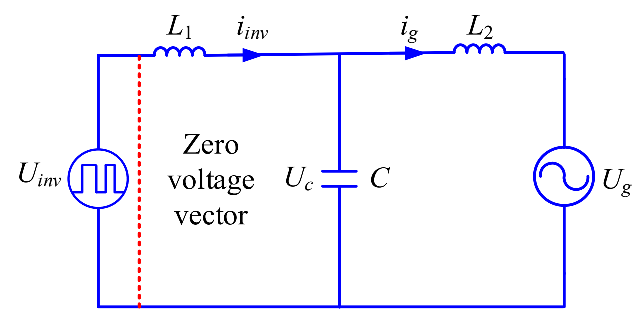

- ❑ Capacitor voltage during zero voltage vectors $U_c = -L_1 \frac{di_{inv}}{dt}$
- ❑ Inverter-side current slope using linear regression $\frac{di_{inv}}{dt} = \frac{\overline{it} - \bar{i}\bar{t}}{\overline{t^2} - \bar{t}^2} = \frac{\frac{1}{n}\sum_{k=1}^{n} i(t_k)t_k - \frac{1}{n^2}\sum_{k=1}^{n} i(t_k)\sum_{k=1}^{n} t_k}{\frac{1}{n}\sum_{k=1}^{n} t_k^2 - \frac{1}{n^2}(\sum_{k=1}^{n} t_k)^2}$

Source: [1] S. He, *et.al.,* "Line voltage sensorless control of grid-connected inverters using multisampling," *IEEE TPEL.*, 2022.

►Line Voltage Sensorless Control

Start-up control

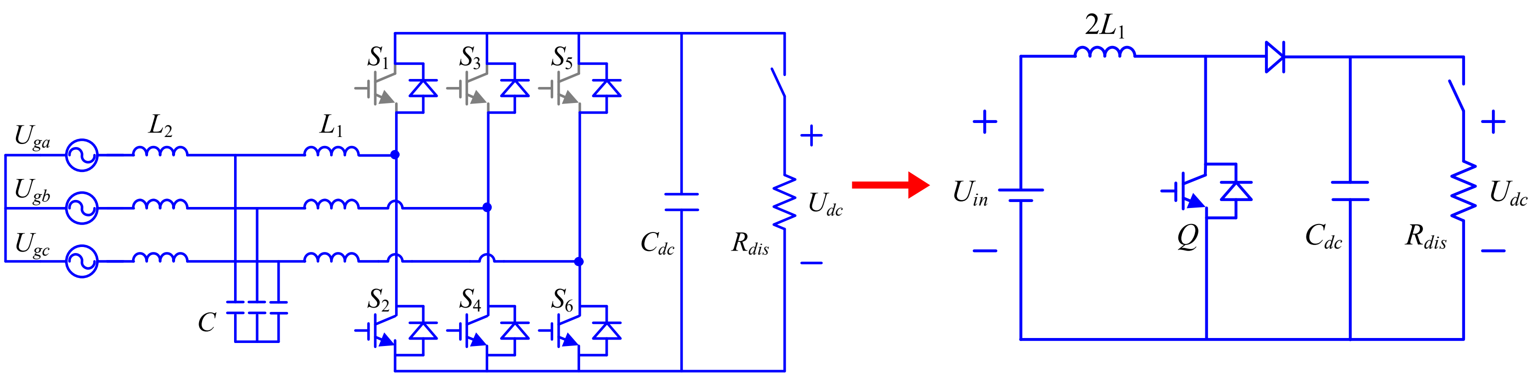

Three phase VSC with locked upper arms

Equivalent boost converter

- ❑ Fundamental start-up current: $L_1 \frac{di_{inv}}{dt} = U_{inv}\sin(\omega_g t + \varphi_0) - U_c \sin(\omega_g t + \varphi_g)$
- ❑ Grid voltage should be known before start-up
- – Injecting zero voltage vectors and control VSC as a boost converter

Source: [1] S. He, *et.al.,* "Line voltage sensorless control of grid-connected inverters using multisampling," *IEEE TPEL.*, 2022.

►Line Voltage Sensorless Control

Start-up process

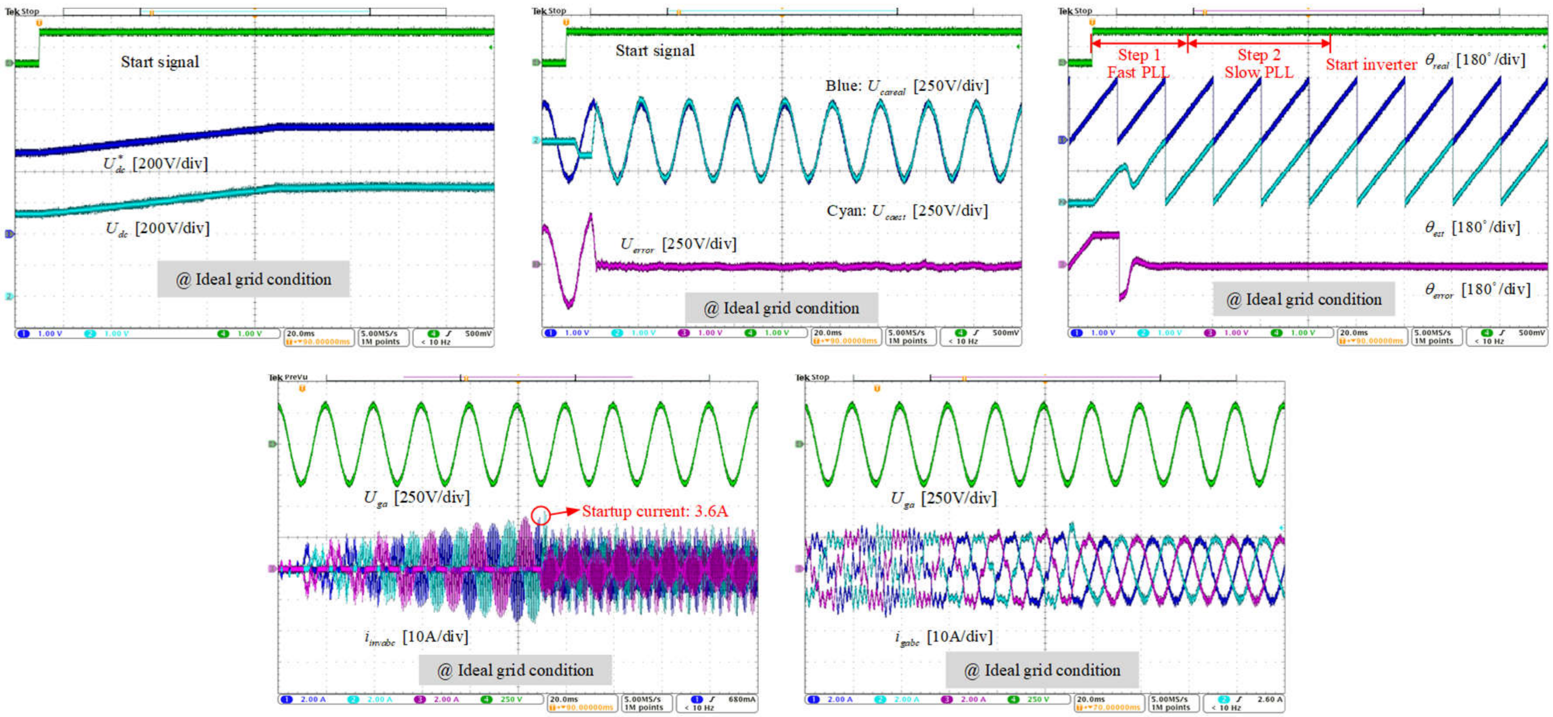

►Line Voltage Sensorless Control

Current reference step response

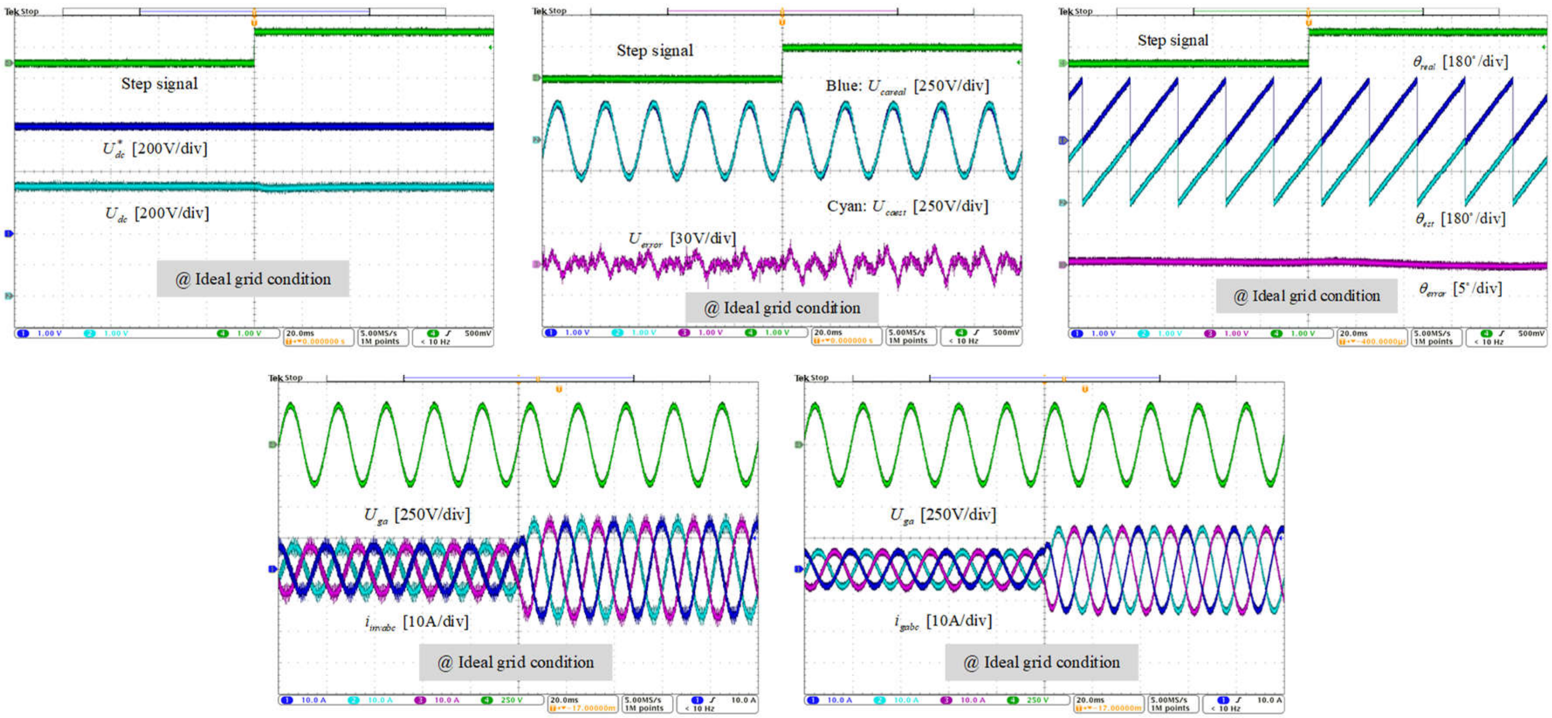

► Conclusion

- ❑ Application of multi-sampling PWM
  - ➢ Multi-sampling PWM mechanism analysis
  - ➢ Ripple filter design
  - ➢ Multi-sampling rate selection
- ❑ Dissipativity enhancement using multi-sampling PWM
  - ➢ Simplified active damping for current/voltage control
  - ➢ Enhanced real-time-update PWM with $0.25T_{sw}$ control delay
- ❑ Grid voltage estimation using multi-sampled current data

► Selected Publications

[1] **S. He**, D. Zhou, X. Wang, and F. Blaabjerg, “Aliasing suppression of multi-sampled current controlled LCL-filtered inverters,” *IEEE Trans. Emerg. Sel. Topics Power Electron*., vol. 10, no. 2, pp. 2411-2423, April 2022.

[2] **S. He**, D. Zhou, X. Wang, and F. Blaabjerg, “Line voltage sensorless control of grid-connected inverters using multisampling,” *IEEE Trans. Power Electron*., vol. 37, no. 4, pp. 4792-4803, April 2022.

[3] **S. He**, D. Zhou, X. Wang, Z. Zhao, and F. Blaabjerg., “A review of multisampling techniques in power electronics applications,” *IEEE Trans. Power Electron.,* vol. 37, no. 9, pp. 10514-10533, Sept. 2022.

[4] **S. He**, D. Zhou, X. Wang, and F. Blaabjerg., “Passivity-based multi-sampled converter-side current control of LCL-filtered grid-connected VSCs, ” *IEEE Trans. Power Electron.,* vol. 37, no. 11, pp. 13848-13860, Nov. 2022.

[5] **S. He**, Z. Yang, D. Zhou, X. Wang, R. De Doncker, and F. Blaabjerg., “Dissipativity robustness enhancement for LCL-filtered grid-connected VSCs with multi-sampled grid-side current control, ” *IEEE Trans. Power Electron.,* 2022.

[6] C. Gao, **S. He***, P. Davari, K. Leung, P. Loh, and F. Blaabjerg, “Passivity-based design of resonant current controllers without involving partial derivative,” *IEEE Trans. Power Electron*., vol. 38, no. 12, pp. 15102-15108, Dec. 2023.

[7] Z. Yang, **S. He***, D. Zhou, X. Wang, R. W. De Doncker, F. Blaabjerg, and L. Ding, “Wideband dissipativity enhancement for grid-following VSCs utilizing capacitor voltage feedforward,” *IEEE J. Emerg. Sel. Topics Power Electron*., vol. 11, no. 3, pp. 3138-3151, June 2023.

Thanks

Shan He
Email: shanhe@ieee.org
Department of Energy
Aalborg University, Denmark

AAU ENERGY AALBORG UNIVERSITY